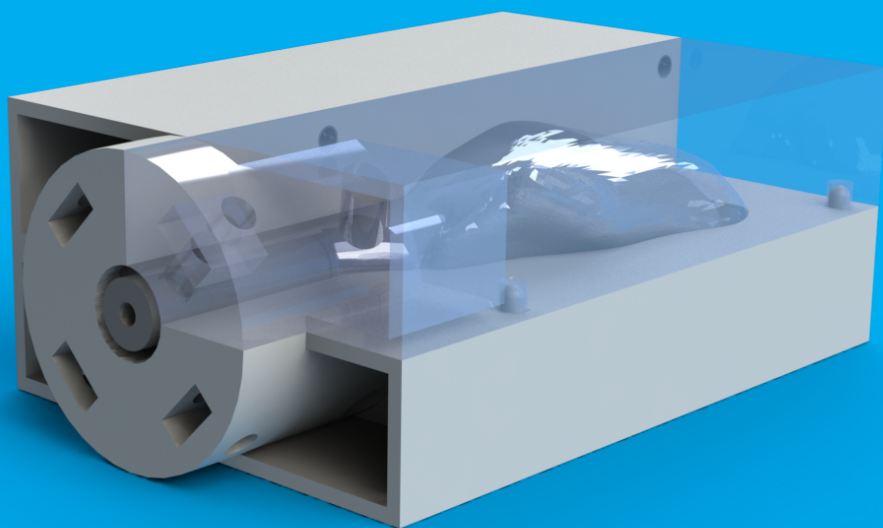


# Creating a Phantom of the Vaginal Cavity for Gynaecological Brachytherapy

P.C. Somerwil





# Creating a Phantom of the Vaginal Cavity for Gynaecological Brachytherapy

by

**P.C. Somerwil**

to obtain the degree of Master of Science  
at the Delft University of Technology,  
to be defended publicly on Friday January 22, 2021 at 09:00 AM.

Student number:	4097998	
Project duration:	July 1, 2020 – January 9, 2021	
Thesis committee:	Prof. dr. J. Dankelman,	TU Delft, supervisor
	Dr. ir. N. J. P. van de Berg,	TU Delft, daily supervisor
	Prof. dr. R. A. Nout,	Erasmus MC



# Preface

The year 2020 has been quite a challenging year, performing a internship and master thesis research during a global pandemic was no easy job. It has brought a lot of changes along the way, especially a lot of working from home. This even resulted in a completed internship at the Erasmus Medical Centre, without ever setting foot inside the hospital. Luckily, working from a lab at the university during my thesis research became a possibility and was so much more rewarding after months of working from home.

Conquering the difficulties of performing your thesis research (during a global pandemic), could I not have done on my own. Therefore, I would like to start by thanking my mother, who has supported me during my complete study. Her support, time, proof-reading and feedback, for both my literature study and this report, have proven vital and saved me from an endless lists of typos and unreadable sentences.

I would also like to thank my brothers and friends for their support during my thesis research, and of course the hours of board games to clear my head after days of performing experiments, working through piles of studies or writing this report.

A huge thank you to Nick, for his guidance as my daily supervisor during my literature study and thesis research. The weekly meetings, guidance, and feedback have proven crucial for the completion of my literature study and this report.

I wish you, the reader, lots of joy with the topic I have studied for over a year.

*P.C. Somerwil  
Delft, January 2021*



# Summary

In this study the production process of a thin-walled double-layered phantom of the vaginal cavity has been developed and tested. This phantom has been used to test strategies for sealing the vaginal cavity, so that ultrasound gel can be used to fill the vaginal cavity improve the visibility of the vaginal cavity in MR-images. The phantom consists of layer mimicking the vaginal wall, and a layer functioning as the surrounding tissue. Since the vaginal wall was considered most important, the study focused on this layer.

PVA-hydrogel and silicone rubber were selected as materials to have their mechanical behaviour tested. In order to evaluate the possibility of using these materials as a material mimicking the bio-mechanical behaviour of the vaginal wall. Due to the surface properties of PVA-hydrogel, a specialized set-up was developed and used to perform tensile testing. Three different types of samples have been compared, using two different set-ups. During tensile testing, Young's moduli were calculated at different amounts of strain. The range for the Young's modulus of 6.7 - 14.4 MPa, resulting from literature, was not matched by any sample during this study. Silicone proved a closer match to the vaginal wall, compared to PVA-hydrogel. Calculated Young's moduli for silicone rubber were between 1.4 - 4.2 MPa, with 0.04 - 0.16 MPa for PVA-hydrogel. Comparing the stress-strain curves instead of the calculated Young's moduli, resulted for silicone rubber samples, in similar stress-strain curves for certain window of strain.

Indentation testing was suggested and tested as an alternative for tensile testing, due to being non-destructive. Which allowed the testing method to be used with developed phantoms. Indentation testing was confirmed as a possible alternative to tensile testing for the verification of mechanical properties of the materials used in this study. Storage by submersion of PVA-hydrogel samples was shown to influence the mechanical properties over time.

Two phantoms have been developed during this study, from PVA-hydrogel and silicone rubber. The shape of these phantoms was based on delineated MR-images which were converted into 3D-structures. The 3D-structures have been used in the development of moulds, in which the phantoms were manufactured. During production, silicone thinner was required to lower the viscosity of the silicone rubber, in order to create the desired thin-walled structure of the vaginal wall. The use of silicone thinner decreases the stiffness of the silicone, when used during manufacturing. This was tested using indentation testing.

To verify the usability of the phantom, the phantom along with samples were placed inside a MR-scanner, to compare intensity differences between the different materials used during this study. The results of this experiment concluded proper differences between different materials could be seen by an untrained person. Differences between different composition of a similar material (silicone rubber and PVA-hydrogel) could be distinguished.

During the final experiment, the phantoms were tested to compare the different methods of sealing of the vaginal cavity. One of the methods, female catheter with a balloon, was discarded due to proving impractical during testing. The other solution (wrapping a ultrasound probe cover around the catheter without a balloon) was compared against the test with just the catheter. The results of testing showed a large difference between the two tests, the amount of filling of the vaginal cavity was improved by, 54.3% and 119.9%, for silicone rubber and PVA-hydrogel phantom respectively.



# Contents

List of Figures	ix
List of Tables	xi
Paper	xv
1 Introduction	1
1.1 Treatment of cervical cancer	1
1.2 Challenges in brachytherapy	1
1.3 Customized needle applicators	2
1.4 Goal	2
2 Mechanical properties	3
2.1 Bio-mechanical properties vaginal tissue	3
2.2 Tissue-mimicking materials	5
2.2.1 Selected material	6
2.3 Methods	6
2.3.1 Experimental set-up iterations	7
2.3.2 Sample shape iterations	8
2.3.3 Data acquisition and processing	8
2.4 Results	9
2.4.1 Adjusting mechanical properties of PVA-hydrogel	9
2.4.2 Different tensile samples	10
2.4.3 Comparing different test set-ups	11
2.4.4 Plastic deformation of samples	12
2.4.5 Pre-conditioning	13
2.5 Discussion	14
2.5.1 Comparison with literature	15
2.5.2 Set-up	16
2.5.3 Sample types	17
2.5.4 Future testing	18
2.6 Conclusion	18
3 Indentation testing	19
3.1 Methods	19
3.1.1 Indentation test 1	20
3.1.2 Indentation test 2	20
3.1.3 Indentation test 3	20
3.2 Results	20
3.2.1 Tensile test 2	21
3.2.2 Indentation test 3	21
3.3 Discussion	22
4 Visibility	23
4.1 Samples	23
4.2 Data acquisition and processing	24
4.3 Future testing	24
5 Phantom production	25
5.1 Digital design	25
5.2 Production process	25

6	Phantom testing	27
6.1	Methods	28
6.1.1	Instrumentation	28
6.2	Results	29
6.3	Discussion	30
6.4	Conclusion	30
7	Discussion	31
7.1	Materials and testing	31
7.2	Indentation testing and sample preservation	31
7.3	Phantom production	31
7.4	Phantom testing	32
7.5	Future testing	32
7.6	Conclusion	32
A	Tensile testing	35
A.1	Pre-load and maximum load data	35
A.2	Tensile test 1 (Pilot)	36
A.3	Comparison PVA-samples	37
A.4	Tensile test 9	37
A.5	Tensile test 10	38
B	Indentation testing	39
B.1	Indentation test 1	39
B.2	Indentation test 2	41
C	PVA-hydrogel & silicone rubber production	43
C.1	Standard procedure PVA-hydrogel production	43
C.1.1	Preparation PVA-hydrogel	43
C.1.2	Preservation of samples	43
C.1.3	Materials & equipment	44
C.2	Data PVA-hydrogel batches	44
C.3	Silicone rubber production	45
C.3.1	Materials & equipment	45
C.4	Data PVA-hydrogel batches	46
D	MRI-Experiment	47
E	Mould design	49
E.1	Mould tensile testing	50
E.1.1	Mould type 1	50
E.1.2	Mould type 2 and 3	51
E.2	Phantom mould	52
F	Clinical background	53
F.1	Stages of cervical cancer	53
G	Phantom testing	55
	Bibliography	57

# List of Figures

1.1	A visual representation of the limitations of most applicators for intracavitary brachytherapy (IC-BT).	2
2.1	Different set-ups used during this study.	7
2.2	Different sample types used during this study.	8
2.3	Mould with samples of sample type 2 prior to demoulding.	8
2.4	Stress-strain plots of the mean sample of each PVA-hydrogel composition.	9
2.5	Stress-strain plots of the mean sample of each sample type.	10
2.6	Comparison of set-up 2 and set-up 3, both set-ups were used with silicone samples.	11
2.7	Stress-strain curves of tensile test 7, showing the influence of prior testing on tensile samples.	12
2.8	Stress-strain curve for a sample with 3x pre-straining prior to the full strain-movement as pre-conditioning.	13
2.9	Range of Young's moduli found for PVA-hydrogel, comparing different sample types and set-ups.	14
2.10	Range of Young's moduli found for silicone rubber, comparing different sample types and set-ups.	14
2.11	Stress-strain curve (Tensile test 10, 1x pre-straining) projected onto the graph from the study of Martins et al. [1]	15
2.12	Stress-strain curve (Tensile test 10, 1x pre-straining) projected onto the graph from the study of Chantereau et al. [2]	16
2.13	Failure point of type 1 samples	17
2.14	Failure point of type 2 samples	17
2.15	Failure point of type 3 samples	17
3.1	Pattern of individual measurements for an average-value measurement	19
3.2	Indentation test	19
3.3	Hardness results from indentation test 1. Each box represents 5 average-measurements which consist of 9 individual measurement.	20
3.4	Results indentation test 2, testing the influence of sample storage over time.	21
3.5	Designed fixation cup for indentation testing.	22
3.6	Rough surface of a PVA-hydrogel sample, this requires the samples to be tested upside-down	22
3.7	Tip of the shore hardness tester.	22
4.1	Shape of the samples used during the MRI-experiment.	23
4.2	MR-image used for intensity calculations, the cyan circles mark the areas used for intensity measurements.	24
5.1	3D-printed insert, in separate parts.	26
5.2	3D-printed insert inside the mold for the vaginal wall.	26
5.3	Mold for vaginal wall filled with silicon rubber.	26
5.4	Insert with vaginal wall after de-molding.	26
5.5	Insert with vaginal wall suspended inside mold for surrounding tissue.	26
5.6	Complete phantom manufactured from silicon rubber.	26
6.1	Pilot experiment using the silicon rubber and PVA-hydrogel phantoms	29
6.2	Overfilling of the silicone phantom, during the experiment using the probe cover.	30
6.3	Overfilling of the PVA-phantom, during the experiment using the probe cover.	30
A.1	Stress-strain curve for the different compositions tested in tensile test 1.	36
A.2	Young's moduli comparison for tensile test 2.	37
A.3	Stress-strain curves: tensile test 9	37
A.4	Start and ending detection done by Matlab-code.	38

---

A.5	Checking accuracy of the detection of the start and ending of the stage movement. . . . .	38
B.1	Comparison of the difference in hardness between samples with similar number of freeze-thaw cycles. . . . .	40
C.1	Production of PVA-hydrogel, pink color is due to the used cooling liquid. . . . .	43
C.2	Mixing container used for the production of silicone rubber. . . . .	45
D.1	Positioning of the sample used in the MR-scanner. . . . .	47
E.1	Dimensions of the different sample types . . . . .	49
E.2	Air defects influencing the shape of tensile sample of type 1. . . . .	50
E.3	Mould for the manufacturing of samples of type 1. . . . .	51
E.4	Mould for the manufacturing of samples of type 2. . . . .	51
E.5	Mould for the manufacturing of samples of type 3. . . . .	52

# List of Tables

1	Contrast differences between the different materials/compositions measured in the MR-image.	xix
2	Results of phantom filling experiment.	xix
2.1	Included studies reporting biomechanical properties of human anterior vaginal wall	4
2.2	Advantages and disadvantages of various materials for phantom production	5
2.3	Overview of the different mechanical tests performed, with sample and set-up settings.	6
2.4	Results Tensile test 2, comparison of the Young's moduli of 6 different compositions of PVA-hydrogel.	9
2.5	Results Tensile test 4 and 5, comparison of the Young's moduli of 6 different tensile types	10
2.6	Comparison between average Young's moduli using set-up 2 and 3, for both silicone rubber and PA-hydrogel.	11
2.7	Comparison of tensile test 7 and 9, comparing the influence of prior testing.	12
2.8	Average Young's moduli for samples with different amounts of pre-conditioning.	13
3.1	Results of indentation test 3, comparing different criteria on their influence on silicone rubber samples.	21
4.1	Differences in signal intensity between the different materials/compositions measured in the MR-image.	24
6.1	Results of phantom filling experiment	29
A.1	Pre-Load and maximum load values for tensile test 1 and 2.	35
A.2	Pre-Load and maximum load values for tensile test 3, 4, 5, 8.	35
A.3	Results of tensile test 1.	36
B.1	Results of indentation test 1. Measurements (M1-M5) are average-value measurements consisting of 9 individual measurements each.	39
B.2	Results of indentation test 2. Measurements are average-value measurements consisting of 9 individual measurements each.	41
C.1	PVA-hydrogel batches tensile test 1-5, and 8	44
C.2	PVA-hydrogel batches indentation test 1 and 2	44
C.3	PVA-hydrogel batches MRI-samples and the phantom	45
C.4	Silicone rubber tensile test 6,7,8 and 10	46
C.5	Silicone rubber batches MRI-samples and the phantom	46
D.1	Results of the intensity measurements performed on the MR-images.	48
E.1	The FIGO stages of the progression of cervical cancer [3]	53
G.1	Weight measurements phantom filling experiment with the silicon phantom and the pilot set-up.	55
G.2	Weight measurements phantom filling experiment using the PVA-hydrogel phantom and the pilot set-up.	55
G.3	Weight measurements phantom filling experiment with the silicon phantom and the catheter without balloon set-up.	56
G.4	Weight measurements phantom filling experiment with the PVA-hydrogel phantom and the catheter without balloon set-up.	56
G.5	Weight measurements phantom filling experiment with the silicon phantom and the condom set-up.	56

G.6 Weight measurements phantom filling experiment with the PVA-hydrogel phantom and the condom set-up. . . . . 56

# Nomenclature

LACC	Locally Advanced Cervical Cancer
IC-BT	IntraCavitary BrachyTherapy
GEC-ESTRO	Groupe Européen de Curiethérapie and the European Society for Radiotherapy & Oncology
HAVW	Human Anterior Vaginal Wall
POP	Pelvic Organ Prolapse
MISIT	Minimally Invasive Surgery and Interventional Techniques
SI	Saline Immersion
SM	Saline Moistened gauze
BMI	Body Mass Index
FIGO	Fédération Internationale de Gynécologie et d'Obstétrique (International Federation of Gynaecology and Obstetrics)



# Paper

# Creating a Phantom of the Vaginal Cavity for Gynaecological Brachytherapy

## Abstract

The goal of this study is to create a phantom which can be used to test strategies for sealing the vaginal cavity, so that ultrasound gel can be used to fill the vaginal cavity improve the visibility of the vaginal cavity in MR-images.

Silicone rubber and PolyVinyl Alcohol(PVA) were tested, to check whether their mechanical properties can be used to mimic the bio-mechanical behaviour of Human Anterior Vaginal Wall(HAVW)-tissue. Both materials were used to produce a phantom. Contrast differences in MR-imaging of PVA-hydrogel and silicone rubber with ultrasound gel and air were measured, to verify proper contrast within a phantom. Both phantoms were used to test sealing strategies.

Young's moduli for HAVW-tissue were obtained from literature, and formed a range(6.7 - 14.4 MPa). Silicon proved a closer match to the HAVW-tissue, compared to PVA-hydrogel. Calculated Young's moduli were between 1.4 - 4.2 MPa (silicone rubber) and 0.04 - 0.16 MPa (PVA-hydrogel). Contrast differences in MR-images were measured between 177.8 and 1585.7, and proved sufficient enough to be spotted by an untrained eye. The sealing strategies using a probe cover surrounding a catheter, showed an increase of 54.3% (silicone rubber) and 119.9% (PVA-hydrogel) of the filling percentage measured. Indentation testing was confirmed as a possible alternative to tensile testing for the verification of mechanical properties.

In this study the production process of a thin-walled double-layered phantom of the vaginal cavity has been developed and tested. The developed phantoms have been used to test strategies for sealing the vaginal cavity. The concept using a catheter surrounded by a probe cover, is considered to improve the sealing of the vaginal cavity.

## Introduction

The release of the GLOBOCAN database in September 2018 has provided worldwide estimates of the incidence, mortality and prevalence rates for all types of cancer. Cervical cancer with 569,847 new cases and 311,365 deaths, have been estimated to accounts for 6.7% of deaths in women due to cancer [4]. The EMBRACE II study [5] presented the current major challenges in the treatment of locally advanced cervical cancer (Stage IB2 and higher [6]). Research at the Delft University of Technology is performed to develop a customized needle applicator which is optimized and manufactured for a single patient. It is the expectation that this solution could reduce treatment-related morbidity and improve quality of life.

The goal of this study is to create a phantom which can be used to test methods for sealing the vaginal cavity, so that ultrasound gel can be used to fill the vaginal cavity improve the visibility of the vaginal cavity in MR-images. Improved visibility of the vaginal cavity, makes the delineation of the region more easy. The delineated region of the vaginal cavity will be used in the development of the customized applicators. Accurate delineation of the region will allow for a close fit between the applicator and the anatomy of the patient.

## Methods

Using a phantom to mimic the sealing of the vaginal cavity, while filling the vaginal cavity with ultrasound gel, will result in expanding of the vaginal cavity. In order to compare different methods for sealing the vaginal cavity, realistic mechanical behaviour during expansion of the phantom is essential.

### Mechanical properties vaginal tissue

Three review studies ([7], [8], [9]) were found. Providing data on the bio-mechanical properties of the different organs (vagina, cervix, uterus, cardinal, uterosacral and round ligaments) present in the pelvic region in monkeys, swines, rats/mice, ewes and human beings. The method of testing was recorded as well. The data of five studies was selected([10], [11], [12], [1], [13]), and used to provide a range for the Young's modulus for HAVW-tissue. The range of the Young's modulus found for HAVW tissue, is 6.7 - 14.4 MPa, representing pre-menopausal 'healthy' tissue up to post-menopausal tissue affected by Pelvic Organ Prolapse (POP).

### Material selection

Silicone rubber and PVA-hydrogel were selected to be used in the development of phantoms. Silicone rubber was selected based on the reduced production time, the great shelf life and dimensional stability (negligible shrinkage/swelling after manufacturing).

Additionally, mechanical properties of the material could be selected based on data from the manufacturer. The selection of PVA-hydrogel was based on adjustability of mechanical properties during manufacturing and tissue-needle interaction. Tissue-needle interaction are selected based on future testing.

### **Samples and set-up**

Due to the slippery surface properties of PVA-hydrogel, clamping was based on shape-locking (instead of friction). This was achieved by letting metal rods pass through the samples. Three different samples were developed and tested during this study, based on examples from literature ([14], [10]). The samples were made by filling 3D-printed moulds, which were designed and converted into STL-files using Solidworks 2019 [Dassault Systèmes, Vélizy-Villacoublay, France]. The STL-files were converted into G-code by Cura 4.7 [Ultimaker, Geldermalsen, the Netherlands], and printed using an Ultimaker 3 [Ultimaker, Geldermalsen, the Netherlands].

The set-up uses an ACT115DL Direct-Drive Linear Actuator [Aerotech inc, Pittsburgh, Pennsylvania, USA]. A Renishaw RGH22S50F61 linear encode [Renishaw, Wotton-under-Edge, UK] is used to measure the location of the platform with  $0.1 \mu\text{m}$  precision. A Soloist CP Controller and PWM Digital Drive [Aerotech inc, Pittsburgh, Pennsylvania, USA] is used to control the movement of the linear stage. The rest of the set-up was custom manufactured for these tensile tests.

### **Data acquisition and processing**

Tensile force data were acquired using a Scaime ZFA 25kg tensile load cell [Scaime, Juvigny, France]. The sensor output was amplified using a Scaime CPJ-CPJ2S analog signal conditioner [Scaime, Juvigny, France] and sent to a computer using a USB Multifunction IO Device NI USB-6008 [National Instruments, Austin, United States]. Data were recorded at a sample rate of 200Hz and saved as txt-files. The movement of the stage was not recorded directly, but calculated during data processing. The moving speed of the stage was kept at the same constant rate of 0.5 mm/s.

The data were processed using Matlab R2019b [Mathworks, Natick, Massachusetts, United States]. The raw force data were first smoothed by a moving average filter, with a kernel size of 50 (window size 0.25s). The start of movement of the stage was detected by scanning for the first sequence of at least 100 consecutive rising values. The end of the movement was detected using the max-function of Matlab.

Detection of start and end of movement were verified visually. Based on the initial position of the stage, and the timestamps from the start and end of the movement, the position of the stage at every timestamp could be determined. Stress and strain conversions were performed using the dimensions of the samples and set-up. The Young's modulus was determined for different amounts of strain. The fit-function of Matlab was used to calculate the Young's modulus, by fitting a first-order polynomial function in a 0.1-strain window.

### **Indentation testing**

Indentation testing was suggested and tested as an alternative for tensile testing, due to being non-destructive. The testing method is more quick and easy, compared to tensile testing. And does not require a specific shape of the sample, which allowed to testing method to be used with developed phantoms. The method was used to compare the differences between different PVA-hydrogel compositions, storage of sample by submersion, and the influence of additives used during manufacturing.

### **MRI visibility**

The phantom should be compatible with the current brachytherapy procedures. MR-imaging is standard imaging method used at the Erasmus Medical Centre, the phantom should have proper contrast with other materials or instrumentation used during MR-imaging. Testing was performed at Erasmus Medical Centre. The test consisted of multiple samples and phantoms being placed inside a MRI-scanner. Intensity measurements were performed to quantify the differences between different materials.

Samples were designed to have a very simple geometric shape, a cube with a cylindrical cavity in the top surface of the cube. The samples were either filled with ultrasound gel or left empty, to simulate the testing of filling the vaginal cavity with ultrasound gel in real patients. During testing eight samples and two phantoms were compared on contrast in the MR-images. Four of the samples were manufactured of PVA-hydrogel, the remaining four samples from silicon rubber. One phantom was manufactured from PVA-hydrogel, the other from silicon rubber.

### **Data acquisition and processing**

Testing was performed using a Optima MR 450w 1.5T scanner [GE Healthcare, Chicago, USA] at the Erasmus Medical Center, which was controlled by a medical specialist. The second coil was placed above the tray, this is standard for the brachytherapy procedure.

Data processing was performed with the provided viewing software [GE Healthcare, Chicago, USA]. Measurements were done by placing a circle in the area which needed to be measured. Each structure was measured using three individual measurements. The circles were placed to minimize the overlap between circles. The circle used for intensity measurements was kept the same size for most of the measurements. For two double layered samples and the VW-layer of both phantoms, smaller circles were used. Each circle provided data on max, average and standard deviation of the intensity within the circle. The average measurements of the three circles are averaged again to a single value, to calculate the difference between the different structures present in the MR-image.

### Phantom production

During the design of the phantom, the shape of the structure mimicking the the vaginal wall being anatomically correct was considered to be more important compared to the shape of the surrounding tissue being anatomically correct. Thus the phantom was designed to consists of hollow vaginal cavity, surrounded by a layer mimicking the vaginal wall, and the vaginal wall was covered by a layer mimicking surrounding tissue.

The 3D structure of the vaginal cavity used, was obtained from the study of Laan et al. [15]. The 3D-structure was developed from delineated MR-images of the vaginal cavity, followed by concatenation of the segmented contours, and surface mesh modeling to create a 3D structure. The 3D model of Laan et al. does not contain a separate 3D structure of the vaginal wall. This structure was created by non-uniform scaling of the vaginal cavity up to an enlarged model, this was done using Solidworks 2019 [Dassault Systèmes, Vélizy-Villacoublay, France]. Using the cavity function the initial 3D structure was subtracted, resulting in a thin walled structure representing the vaginal wall. This structure was used in the development of the moulds used for the production of the phantoms.

### Production process

The production of a phantom starts with 3D-printing a water-soluble PVA-insert, with the shape of the vaginal cavity. This insert can be dissolved when the manufacturing process of the other layers of the phantom are completed. The insert is inserted into a mould, the space between the insert and the mould is equal to the 3D-modeled vaginal wall. This mould is 3D-printed of PolyLactic Acid (PLA), the mould consists of 4 separate parts to fit around the insert. The mould has a small container on the top of each part

of the mould, a sloping channel connects the container to the inside of the mould. These containers function as a filling reservoir for the mould, which is required due to the high viscosity of the silicon rubber.

After the curing of the silicon rubber or the completion of the freeze-thaw cycles for PVA-hydrogel, the insert surrounded by the vaginal wall is removed from the mould. And is suspended in an acrylic container, for the manufacturing of the layer of the surrounding tissue. The layer mimicking the surrounding tissue was developed as an uniform layer, the biomechanical properties of this layer remain constant. In order to simplify production and handling of the phantom the outer shape of this layer was chosen to be a rectangular block.

### Phantom testing

The procedure of filling the vaginal cavity with ultrasound gel, while MR-images are made, has already been performed at the Erasmus Medical Center. The main difficulty found during experimental trails, was the leakage of the ultrasound gel during the MR-procedure. During my internship at the Erasmus MC prior to this study, I have studied this problem and developed a few concepts which could resolve the leakage. These concepts will be tested in this experiment.

The developed phantoms (PVA-hydrogel and silicon rubber) are placed inside a container on a scale (Kern EMS 6K1 [Kern & Sohn GmbH, Balingen, Germany]). The phantom is placed under a 20°-angle with the horizontal axis to match the anatomy of the patient. The phantom is then filled with ultrasound gel, some overfilling is performed to remove any air pockets present inside the phantom. The set-up is left for 15 minutes, so any further leakage of ultrasound gel could occur. After 15 minutes, the filling device is clamped shut. The phantom is removed and was weighted, using a different scale (Kern EMB 600-2 [Kern & Sohn GmbH, Balingen, Germany]), to compare with the measurement performed prior to the experiment. Additional measurements are performed to verify the results.

The experiment was repeated using the different concepts. A pilot was performed prior to other tests to check the testing protocol. Equipment presented below were provided by the Erasmus Medical centre. Tests were performed using a 60ml Plastipak catheter tip syringe [BD, New Jersey, USA], and supragel ultrasound gel [LCH medical products, Paris, France]. Concepts were compared with the base test using a female catheter,  $\varnothing$ : 4.7mm (14Ch),

length 18cm [Medicoplast International GmbH, Illingen, Germany]. The first concept used a Rusch Gold balloon catheter,  $\varnothing$ 5.3mm (16Ch), 5-15mL [Teleflex, Pennsylvania, USA]. The balloon was filled using a 10mL Luer tip (6%) emerald syringe [BD, New Jersey, USA]. The second concept used the same catheter as the base test, with a ultracover ultrasound probe cover (34 x 200 mm) [Ecolab, Minnesota, USA] wrapped around approximately the first 5 cm of the catheter. The probe cover was fixated using two rubber bands twisted around the cover and catheter tube.

## Results

During tensile testing, different sample types and setups were used, to eliminate unwanted failure mechanisms of the samples. After all tensile tests were completed, the Young's moduli for PVA-hydrogel and silicone rubber samples were calculated over a range of strain, 1.1-2.0 and 1.1-1.6 respectively. All tested samples were outside the range obtained from literature (6.7 - 14.4 MPa). Silicon proved a closer match to the vaginal wall, compared to PVA-hydrogel. Calculated Young's moduli for silicone rubber were between 1.4 - 4.2 MPa, with 0.04 - 0.16 MPa for PVA-hydrogel. Preconditioning was observed to influence the mechanical behaviour of the tensile samples. The mechanical behaviour became more non-linear when samples had been tested prior. Testing the samples with a pre-strain of 0.175 did not show a clear difference for higher levels of strain.

### Indentation testing

Indentation testing showed similar trends between different PVA-hydrogel compositions as observed during tensile testing. Therefore, it was confirmed as a possible alternative to tensile testing for the verification of mechanical properties. Samples tested over a 3-week period showed increased hardness over time as a result of sample storage by submersion in water.

### MRI testing

During the experiment the intensity differences between air, ultrasound gel, two types of silicone rubber and two compositions of PVA-hydrogel were compared in MR-images. The contrast was clear enough for an untrained eye to be spotted between all different previously mentioned materials. All contrast differences can be seen in table 1. Largest differences observed were between high PVA-content PVA-hydrogel and air, smallest differences between Silicon 940 and air. The contrast differences of the phantoms are not displayed, due to presence of air pockets and the fine structures which made the measure-

ments more susceptible to such disturbances.

Table 1: Contrast differences between the different materials/compositions measured in the MR-image.

Combination	Contrast difference
Silicon 940 - Air	177.8
Silicon 940 - UG	406.3
Silicon 18 - UG	337.9
Silicon 940 - Silicon 18	158.5
PVA 14%, 3C - Air	1585.7
PVA 14%, 3C - UG	667.1
PVA 8%, 2C - UG	287.0
PVA 14%, 3C - PVA 8%, 2C	283.6

UG: ultrasound gel

### Phantom testing

During the phantom testing both phantoms (silicone and PVA-hydrogel) were tested, results are shown in table 2. Estimated volume of the phantoms was based on the volume of the PVA-insert used during the manufacturing of each phantom. The base test showed overfilling of the PVA-hydrogel phantom to be possible, which was not the case for the silicone rubber phantom. The test with the first concept (balloon catheter) was aborted after multiple attempts. The second concept (catheter with probe cover) proved successful. The results showed a large difference compared to the base test, the amount of filling of the vaginal cavity was improved by, 54.3% and 119.9%, for silicone rubber and PVA-hydrogel phantom respectively.

Table 2: Results of phantom filling experiment.

	Volume (V) [mL]	Estimated V [cm <sup>3</sup> ]	Filling % [%]
<b>Pilot</b>			
Silicone	21.70	24.0	90.4%
PVA	27.10	28.1	96.4%
<b>Base test: catheter</b>			
Silicone	20.92	24.0	87.2%
PVA	38.03	28.1	135.3%
<b>Balloon catheter</b>			
Silicone	-	-	-
PVA	-	-	-
<b>Catheter surrounded by probe cover</b>			
Silicone	33.97	24.0	141.5%
PVA	71.72	28.1	255.2%

## Discussion

Samples closest to the range of HAVW-tissue from literature, had been subjected to straining prior to tensile testing, either by prior tensile test(s) or by deliberated pre-conditioning. The effect of pre-conditioning of tensile samples has only been tested with silicone rubber samples, and the testing has been limited. Additional testing could provide information on whether reusing of phantoms is possible and what differences in mechanical behaviour it will cause. Pre-conditioning of tensile samples can be easily performed and controlled, for a phantom this will prove more difficult.

During the production of the silicone rubber phantom, silicone thinner was required. It was used to lower the viscosity of the silicone rubber, in order to create the desired thin-walled structure of the vaginal wall. The use of silicone thinner decreases the stiffness of the silicone, when used during manufacturing. This was tested using indentation testing.

Both the effects storage by submersion of samples in water and use of silicone thinner during manufacturing have been measured using indentation testing. However, these effects have not yet been tested via tensile testing.

The MRI testing has already compared the contrast differences between materials used, and the ultrasound gel and air which will be present during testing. For future testing an additional material, or a variety of materials, should be introduced to represent the customized applicator. And would be either a type of filament or a type of resin.

During phantom testing, the concept using a female balloon catheter, was discarded due to proving impractical during testing. Future testing would include performing the experiment again, and placing the phantom inside a MRI-scanner after the filling process is completed. Using the MR-images, the ability of the probe cover to adapt to the shape of the vaginal cavity could be confirmed.

# 1

## Introduction

Cervical cancer is one of the most common types of cancer for women. The release of the GLOBOCAN database in September 2018 has provided worldwide estimates of the incidence, mortality and prevalence rates for all types of cancer [4]. Cervical cancer is the fourth most common type of cancer in regard to incidence, mortality and prevalence rate cancer in women [6]. For cervical cancer, 569,847 new cases and 311,365 deaths, have been estimated to have occurred in 2018 world wide. Cervical cancer accounts for 6.7% of deaths in women due to cancer.

### 1.1. Treatment of cervical cancer

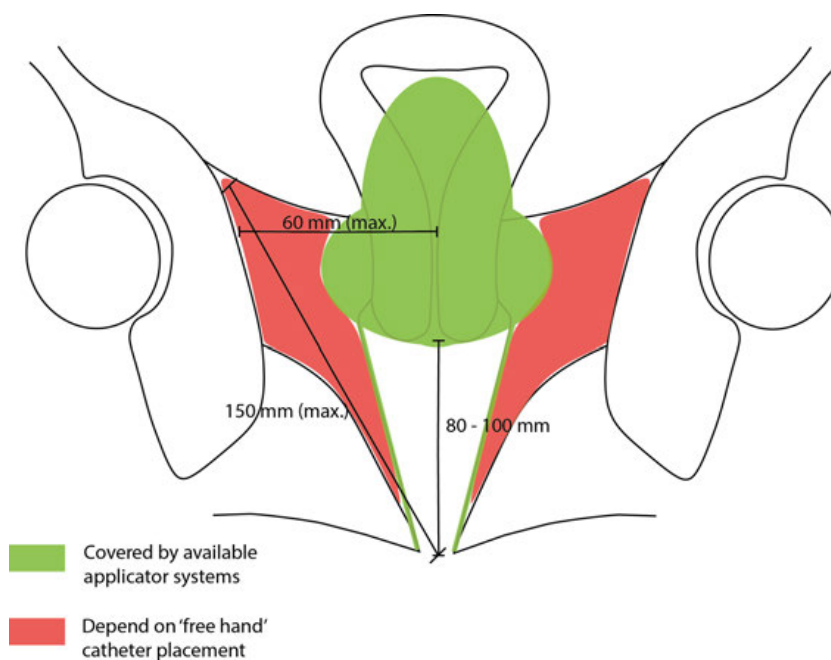
There are several options for the treatment of cervical cancer, the five standard types of treatment are: surgery, radiation therapy, chemotherapy, targeted therapy, and immunotherapy. Different types of treatment are often used concurrently to achieve the best treatment possible for the patient. The stage of the cancer is often the decisive factor for the types of treatment available for the patient.

Especially with higher stage and/or high spread cancer, the selection of types of treatment gets reduced. Stage IB2 and higher stages in cervical cancer are referred to as Locally Advanced Cervical Cancer (LACC) [3], a more detailed overview of the different stages of cervical cancer can be found in Appendix F. The treatment of LACC often consists of radiation therapy, both external and internal. These two types of radiotherapy are often used concurrent in the treatment of LACC. Internal radiation therapy, also known as brachytherapy, functions by placing a radioactive source in close proximity of the tumour.

### 1.2. Challenges in brachytherapy

The Groupe Européen de Curiethérapie and the European Society for Radiotherapy & Oncology (GEC-ESTRO), the European expert group on (image guided adaptive) brachytherapy has initiated the EMBRACE II study [5]. This study states that the current major challenges in the treatment of locally advanced cervical cancer are: local control in advanced tumours, treatment-related morbidity and quality of life, distant metastatic spread, and selection of patients for additional systemic treatment. This first mentioned challenge, local control in advanced tumours, is mostly dependent on the current available applicators.

This challenge is visualized in Figure 1.1, the area shown in green can be properly radiated using the current standard applicators. The areas shown in red, require additional invasive instrumentation in order to receive sufficient dosage. The spread of LACC is often near or over the border of the green region, e.g. stage IIB and higher are defined by tumour spread to the parametrial area. Treatment of LACC will require the use of interstitial needles. These needles can either be placed using outward curving guide channels in advanced applicators, or require to be placed 'free-hand' by a medical specialist which reduces control and repeatability and is highly dependant on the skills of the medical specialist.



The green area is covered well by most applicators, the areas shown in red represent the areas of limitation. The areas not properly covered are the left and right parametria and the lower part of the vagina. Cancer growth in the parametrial area is defined as stage IIB and spread to the lower part of the vagina is defined as stage III as can be seen in Appendix F.

Figure 1.1: A visual representation of the limitations of most applicators for intracavitary brachytherapy (IC-BT).

### 1.3. Customized needle applicators

Advanced applicators are required to offer sufficient additional coverage compared to the more common applicators. This additional coverage is achieved through the presence of additional guide paths for interstitial needles, and having more oblique needle guide paths compared to other applicators. Using these advanced applicators give medical specialists a wider selection in needle locations to improve target coverage and dose distribution.

Since the advanced applicator is developed to be used for a large group of patients, the applicator will never be optimal for a single patient. To solve this problem, research at the Delft University of Technology is performed to develop a customized needle applicator which is optimized and manufactured for a single patient. It is the expectation that this solution could reduce treatment-related morbidity and improve quality of life.

### 1.4. Goal

The goal of this study is to create a phantom which can be used to test strategies for sealing the vaginal cavity, so that ultrasound gel can be used to fill the vaginal cavity improve the visibility of the vaginal cavity in MR-images. Improved visibility of the vaginal cavity, makes the delineation of the region more easy. The delineated region of the vaginal cavity will be used in the development of the customized applicators. Accurate delineation of the region will allow for a close fit between the applicator and the anatomy of the patient.

# 2

## Mechanical properties

Using a phantom to mimic the sealing of the vaginal cavity, while filling the vaginal cavity with ultrasound gel, will result in expanding of the vaginal cavity. In order to compare different methods for sealing the vaginal cavity, realistic mechanical behaviour during expansion of the phantom is essential. In this chapter the process of mimicking the bio-mechanical properties is described. Starting with a literature study, gathering data on the bio-mechanical properties of the pelvic region of women, with a focus on the vaginal wall. This is followed by an overview of materials considered to be used in this study. Finally the performed mechanical tests are reported and discussed.

### 2.1. Bio-mechanical properties vaginal tissue

Three review studies were found by Baah-Dwomoh et al. [7], Eberhart et al. [8], and Ruiz-Zapata et al. [9], providing data on the bio-mechanical properties of the different organs (vagina, cervix, uterus, cardinal ligament, utero-sacral ligament and round ligament) present in the pelvic region in monkeys, swines, rats/mice, ewes and human beings. Method of testing to determine the bio-mechanical properties studies was also recorded, as well as the influence of certain factors (pregnancy, parity, menopause, prolapse) on these biomechanical properties.

Results were included when studies used human anterior vaginal wall (HAVW) tissue, collected data on the Young's modulus of the tissue by performed tensile tests. Studies focused on developing a model for the mechanical behaviour of HAVW were excluded. The included studies can be found in Table 2.1. Most studies focussed on patients suffering from pelvic organ prolapse, comparing the differences in biomechanical properties to healthy subjects. Due to the (potential) destructive nature of tensile testing, in vivo data were not available.

The study by Goh [10] compared pre- and postmenopausal tissue of women suffering from pelvic organ prolapse (POP). Tissue samples were collected during prolapse repair surgery. The samples collected were longitudinal strips, originally from the anterior wall of the vagina. Samples were stored wrapped in saline-soaked gauze and frozen at  $-70^{\circ}\text{C}$ . Prior to testing the samples were thawed for 1 hour at room temperature, and were trimmed into a rectangular shape (50 x 10mm). Loops were made at both ends by securing the sample to itself using sutures and tissue glue. During testing the samples were surrounded by a layer of paraffin oil to prevent dehydration, the surrounding temperature was kept at  $37^{\circ}\text{C}$ . Young's moduli were collected at three chosen amounts of stress for both the pre- and postmenopausal tissue.

Lei et al. [11] broadened the study of Goh, by adding healthy control subjects to the group of patients and comparing the bio-mechanical properties for different levels of POP [16]. The samples were collected, stored and tested similar to the study of Goh, the size of the tissue samples was halved in both dimensions (25 x 5mm). The average time between sample collection and testing was 24 hours.

The study by Zimmern et al. [12] compared two methods of sample preservation: saline immersion and wrapping in gauze moistened with saline. Immersion in saline caused overhydration of the samples which mechanically weakened the samples. The higher Young's modulus value found for 'healthy' tissue compared to the POP-affected tissue does conflict with the conclusion of the other studies.

Martins et al. [1] compared multiple criteria for their influence on the biomechanical properties of the HAVW. The study included 15 'healthy' tissue samples, the results of these 'healthy' samples appear to be not separated from the POP-samples in the comparison of different variables in the study. Every variable other than presence of POP, could be influenced by the unequal distribution of 'healthy' tissue between the compared groups, thus only the comparison between 'healthy' tissue and POP-affected tissue is included and shown in Table 2.1.

Lopez et al. [13] compared patients suffering from POP and grouped the patients based on having a body mass index below or above 25. In this study preconditioning of the tissue samples was also preformed and studied. The results of the study also report non-maximum tensile moduli for 10% and 25% of strain.

Table 2.1: Included studies reporting biomechanical properties of human anterior vaginal wall

Study	N	Group, group size	Results
Goh et al, 2002 [10]	18	POP-pre, 8	8.3 ± 1.1 Mpa @0.2MPa
			9.5 ± 1.3 MPa @0.3MPa
			11.5 ± 1.5 MPa @0.4 MPa
		POP-post, 10	9.8 ± 1.4 Mpa @0.2MPa
			11.3 ± 1.7 MPa @0.3MPa
			14.4 ± 2.0 MPa @0.4 MPa
Lei et al, 2007 [11]	23	Non-POP-pre, 14	6.7 ± 1.5 MPa
		POP-pre, 9	9.5 ± 0.7 MPa
	20	Non-POP-post, 8	10.3 ± 1.1 MPa
		POP-post, 12	12.1 ± 1.1 MPa
	21	POP mild, 8	9.4 ± 0.7 MPa
		POP mod, 6	11.6 ± 1.2 MPa
Zimmern et al, 2009 [12]	42	Non-POP, 3	10.2 ± 3.9 MPa
		POP-SI, 16	4.4 ± 2.8 MPa
		POP-SM, 23	8.4 ± 4.8 MPa
Martins et al, 2013 [1]	55	Non-POP, 15	6.9 ± 1.1 MPa
		POP, 40	13.1 ± 0.8 MPa
Lopez et al, 2015 [13]	28	POP-post BMI<25, 13	1.9 ± 0.8 MPa
		POP-post BMI>25, 15	3.7 ± 2.7 MPa

POP: pelvic organ prolapse; -pre: pre-menopausal; -post: post-menopausal; Non-POP: no pelvic organ prolapse; SI: saline immersion, SM: saline moistened gauze; BMI: body mass index

Most studies concluded that POP increases the stiffness of the HAVW tissue. The results of these studies are combined into a single range, 6.7 - 14.4 MPa. This range represents HAVW tissue varying from pre-menopausal healthy patients (lower part of the range) up to post-menopausal patients with tissue severely affected by POP (upper part of the range). For this range the results of the saline immersion group of Zimmern et al. [12] are excluded, since this method of tissue preservation was not recommended by their own study. The results of the study of Lopez et al. [13] are excluded as well due to their great deviation from the results of the rest of the studies. Creating a phantom with a measured Young's modulus within this range (6.7 - 14.4 MPa) would be considered to accurately mimic HAVW-tissue. Possible materials and tensile testing of these materials is discussed in the next sections.

## 2.2. Tissue-mimicking materials

The previous section has given a target range for the preferred bio-mechanical properties of the tissue. In this section the choice of material for the phantom is discussed. This discussion will be based on properties other than the Young's modulus of the material. The materials discussed were selected based on being often discussed in literature or by previous experience with the use of the material by the MISIT (Minimally Invasive Surgery and Interventional Techniques) research group of the Technical University of Delft. The phantom will initially only be used for comparing methods to seal the vaginal cavity while being filled with ultrasound gel. The phantom could be used, during the development of customized applicators, to test the placement of interstitial needles.

### Polyvinyl alcohol hydrogel (PVA-hydrogel)

PVA-hydrogel is often used in biomedical applications [17],[18]. The material is also used in different studies of the MISIT group, mainly for needle-tissue interaction [19]. Advantages of the material include: easy production of samples, the needle-tissue interaction mimicking properties, and the mechanical properties can be altered by adjusting weight percentage of PVA and number of freeze-thaw cycles. Disadvantage of the use of PVA hydrogel includes the following: the production is quite time consuming when multiple (>3) freeze-thaw cycles are required, the forming of cross-links (which provides the strength of the material) is random which has a negative impact on consistency. Furthermore, the material is prone to dehydration so it should be preserved by submersion in water. The method of preservation of the sample leads initially to swelling of the material and shrinkage over a longer time of storage.

### Silicone rubber

Silicone rubber has a better shelf life compared to PVA hydrogel, and does not require the same preservation method (submerging in water). The manufacturing process is often faster and requires almost no specialized equipment. A disadvantage of the use of silicone rubber is that altering the mechanical properties of the material is not possible without the purchase of different raw materials. However alternative raw materials can be purchased easily with mechanical data sheets available by the manufacturers. Another large disadvantage of this material is the surface friction of the material which will not mimic needle-tissue interaction closely. The shrinkage of the material after manufacturing is negligible.

### Gelatin

Gelatin was used by Nattagh et al. to develop a phantom for image-guided BT needle insertion, placing a suture on the vaginal wall, and suturing the cervical lip [20]. The production of gelatin samples or phantoms is very cheap, not complicated and does not require specialized equipment. The shelf life of the material is quite limited, and the material is prone to the growth of mold. To reduce the change of mold growth, samples need to be stored refrigerated and in water, which causes swelling of the samples. The mechanical properties of the material can be adjusted by altering the manufacturing process, but is expected to be less compared to the PVA-hydrogel. Agar is very similar in terms of advantages and disadvantages compared to gelatin, this material is plant based instead of made from animal products.

Table 2.2: Advantages and disadvantages of various materials for phantom production

	PVA-hydrogel	Silicone rubber	Gelatin
Costs raw materials	+ -	-	++
Production time	-	+	+
Shelf life after production	+	++	--
Dimensional stability	-	++	-
Adjustability mechanical properties	+	++	-
Needle-tissue interaction	++	--	+

Dimensional stability is defined as a material not being prone deformation (swelling or shrinkage).

### 2.2.1. Selected material

Both silicone rubber and PVA-hydrogel were selected to be used in this study. Silicone rubber was selected based on the reduced production time combined with the great shelf life and dimensional stability. Additionally, selection could be performed more easily since the mechanical properties of the material are often known by the manufacturer. The selection of PVA-hydrogel was mainly based on the last two criteria from Table 2.2. Since the mechanical properties play a vital role in the testing of the sealing methods. In future testing as well, involving the placement and fixation of the customized applicator will require accurate mimicking of the elastic properties. Needle-tissue interactions will be the main focus while testing customized applicators on the correct guidance of interstitial needles.

### 2.3. Methods

In this section the mechanical testing will be described. The samples types, specialized set-up, and different tests that have been manufactured or performed during this study are shown. Uniaxial tensile testing was chosen as the method of testing of the mechanical properties of the materials, because this is the most prevalent method of testing found in literature as concerned to testing vaginal tissue.

Due to the slippery surface properties of PVA-hydrogel, clamping was based on shape-locking (instead of friction). This was achieved by letting metal rods pass through the samples. Three different samples were developed and tested during this study, the differences are further elaborated in subsection 2.3.2. The samples were made by filling 3D-printed moulds, which were designed and converted into STL-files using Solidworks 2019 [Dassault Systèmes, Vélizy-Villacoublay, France]. The STL-files were converted into G-code by Cura 4.7 [Ultimaker, Geldermalsen, the Netherlands], and printed using an Ultimaker 3 [Ultimaker, Geldermalsen, the Netherlands]. The development of these moulds is described in Appendix E.

A specialized set-up is presented in subsection 2.3.1. The equipment used for the data acquisition and methods for data processing are described in subsection 2.3.3. A total of ten mechanical tests was performed with this set-up, a quick overview of this can be found in Table 2.3.

The first test was performed as a pilot to verify the testing protocol. The second test compared a range of different PVA-compositions to measure the influence of production variables on the tensile strength of the samples. Tensile test 3-5 involved two new sample types (2 and 3). During tensile test 6, silicone rubber samples were evaluated. The following tests (7 & 8) introduced a new set-up (with a method of clamping) and tested both silicone rubber and PVA-hydrogel samples. The final two tensile tests (9 and 10) were only performed with silicone rubber samples. Tensile test 9 focussed on the influence of prior testing of a sample, by re-using a set of samples and testing the set under similar conditions. The last tensile test compared the influence of pre-conditioning of the sample by applying pre-straining prior to fully stretching the sample. Samples were divided into three groups: no pre-conditioning, single 17.5% pre-straining, and triple 17.5% pre-straining, with the first group consisting of four samples and the other groups of three samples. Pre-straining was performed at the same rate as the full strain (0.5 m/s).

Table 2.3: Overview of the different mechanical tests performed, with sample and set-up settings.

Name	Material	W% PVA	Cycli	Silicone	Sample type	Set-up	Purpose
Test 1	PVA	10, 12	2, 3, 4	-	1	2	Pilot
Test 2	PVA	10, 12, 14	2, 3, 4	-	1	2	Different compositions of PVA
Test 3	PVA	12	2	-	2	2	Testing sample type 2
Test 4	PVA	12	2	-	1, 2	2	Comparison sample type 1 & 2
Test 5	PVA	12	2	-	3	2	Testing sample type 3
Test 6	Silicone	-	-	940	3	2	Tensile test silicone
Test 7	Silicone	-	-	940	3	3	Silicone, set-up 3
Test 8	PVA	12	2	-	3	3	PVA, set-up 3
Test 9	Silicone	-	-	940	3	3	Plastic deformation
Test 10	Silicone	-	-	940	3	3	Pre-conditioning

### 2.3.1. Experimental set-up iterations

The set-up uses an ACT115DL Direct-Drive Linear Actuator [Aerotech inc, Pittsburgh, Pennsylvania, USA]. A Renishaw RGH22S50F61 linear encode [Renishaw, Wotton-under-Edge, UK] is used to measure the location of the platform with  $0.1 \mu\text{m}$  precision. A Soloist CP Controller and PWM Digital Drive [Aerotech inc, Pittsburgh, Pennsylvania, USA] is used to control the movement of the linear stage. The rest of the set-up was custom manufactured for these tensile tests.

#### Set-up 1

The first developed set-up can be seen in Figure 2.1a. Alignment of the set-up was done by movements indicated as A and D in the figure. Movement along the X-axis (A) adjusts the bottom part of the set-up to match the top part of the set-up. The top of the set-up can be adjusted along the Y-axis (D) to match the bottom part of the set-up. The set-up needs to be sent to the home position after each run. To ensure clearance for this movement, the table(3) and lower clamp(6) can be lowered by removing the bolts through the legs(2). This movement is marked by B in the figure. By adjusting the pre-load nut(5), the pre-load can be adjusted.

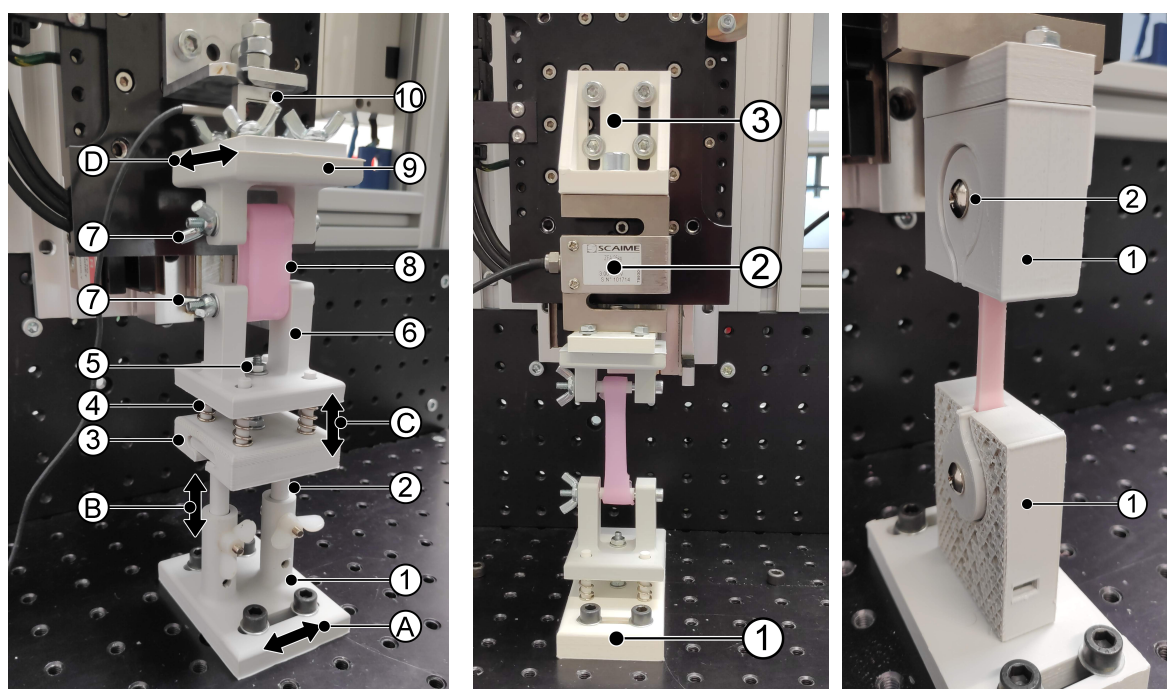
This set-up has not been used, the leg construction proved to be not rigid enough. Additionally, the force sensor used was not rated for forces above 20N, a higher rated (forces above 20N) force sensor was required, for which the set-up required readjustments.

#### Set-up 2

This set-up eliminated the need for the leg construction by redesigning the set-up to ensure clearance. This updated set-up can be seen in Figure 2.1b, the table from set-up 1.0 now serves the function of the base plate as well. The force sensor(2) required a new connection block(3) to be attached to the linear stage.

#### Set-up 3

The final set-up changed the method of fixation from rod clamping to fully form-fitted fixation of both ends of the sample, leaving only the narrow part of the sample not fixated. This was done to eliminate the failure of the samples near their fixation points.



1: Base plate, 2: Leg(s), 3: Table, 4: Spring,  
5: Pre-load nut, 6: Lower clamp, 7: Sample lock bolt,  
8: Sample, 9: Clamp (upper), 10: Force sensor.  
Set-up can be adjusted by A,B,C, and D.

(a) Overview of set-up 1.

1: This set-up has the table connected directly to the base of the stage.  
2: A larger tensile load cell was added.  
3: New connector for the load cell.

(b) Overview of set-up 2.

1: Two end-blocks were manufactured, which fully enclose the fixation endings of a sample.  
2: Cover to prevent deformation within end-blocks.

(c) Overview of set-up 3.

Figure 2.1: Different set-ups used during this study.

### 2.3.2. Sample shape iterations

During mechanical testing three different samples have been tested. The three different types of sample are described below. Dimensions of each sample type can be found in Appendix E. The adjustments and explanation for the different sample type is discussed in section 2.4.

#### Type 1

The first type was designed as an '0'-shape, this shape was designed after an example from literature [14] recommended by a Biomaterials & Tissue Biomechanics expert (Delft University of Technology).

#### Type 2

The second type was designed with a single-strand design instead of a double-strand. The shape of this sample mimics the shape of the sample used by Goh [10]. Instead of reattaching the ends of the strip to create loops, the shape of the mould creates these loops. The distance between the holes for the rods is increased, so the sample is not strained prior to the beginning of the test.

#### Type 3

This type was similar in shape to type 2 samples, with some changes in the thickness of the different parts of the sample. The thickness, around the hole through which the pulling rods will be inserted, is increased. And the thickness of the narrow part of the sample is decreased.



Figure 2.2: Different sample types used during this study.



Figure 2.3: Mould with samples of sample type 2 prior to demoulding.

### 2.3.3. Data acquisition and processing

Tensile force data were acquired using a Scaime ZFA 25kg tensile load cell [Scaime, Juvigny, France], placed between the upper clamp and the fixation block (connected to the linear stage). The sensor output was amplified using a Scaime CPJ-CPJ2S analog signal conditioner [Scaime, Juvigny, France] and sent to a computer using a USB Multifunction IO Device NI USB-6008 [National Instruments, Austin, Texas, United States]. Data were recorded at a sample rate of 200Hz and saved as txt-files. The movement of the stage was not recorded directly, the moving speed of the stage was kept at the same constant rate between all different tensile tests of 0.5 mm/s. The position of the stage for length calculations was performed later in the data processing step.

Force data from the load cell along with timestamps, were saved in txt-files. The data were processed using Matlab R2019b [Mathworks, Natick, Massachusetts, United States]. Multiple files could be processed at the same time, separating different batches of material. The raw force data were first smoothed using a moving average filter, movmean, with a kernel size of 50. At the sample rate of 200Hz, this results in smoothing over a window of 0.25s. The start of movement was determined by scanning the filtered force data for a sequence of at least 100 consecutive rising values. The end of the movement was detected using the max-function of Matlab. Based on the initial position of the stage, and the timestamps from the start and end of the movement, the position of the stage could be determined. Stress and strain conversions were performed using the dimensions of the samples and set-up. The Young's modulus was determined for different amounts of strain. The fit-function of Matlab was used to calculate the Young's modulus, by fitting a first-order polynomial function in a 10%-strain window (e.g. the M60% was determined by fitting a curve to the stress value from 55-65% of strain). The filtered data were plotted with indicated beginning and ending of the movement for visual confirmation of correct detection. The stress-strain curves of all individual samples were plotted as well. The calculated Young's moduli were saved into a table-structure and exported.

For the pre-conditioning dataset the script was slightly altered to adapt for multiple starts and end of the movement. Instead of the max-function, the findpeaks-function, with the minimal peak width set to 1000 and the minimal peak distance of 100, was used to determine the ends of the movement. To detect the different starts of movement, the previous described method was used starting from the beginning of the dataset and detecting only the first 100 consecutive rising values. For the next start the starting point was shifted to the detected end points of the movement by the findpeaks-function.

## 2.4. Results

In this section the results of the tensile tests are presented. The curves shown in the stress-strain curves were based on the closest match with the mean values for the found Young's moduli for that particular test. Data on pre-load and max load can be found in Appendix A, but these data were not used for the matching of samples.

### 2.4.1. Adjusting mechanical properties of PVA-hydrogel

Tensile test 2 (sample type 1, set-up 2) was performed to verify that the mechanical properties of PVA-hydrogel can be easily adjusted by changing the weight-percentage (%-PVA) of PVA used or number of freeze-thaw cycles used during the manufacturing of the samples. In the test six different compositions of PVA-hydrogel were compared, chosen %-PVA (12%, 14%, and 16%) and number of cycles (2 and 3). Each composition consists of ten individual samples, except the batch 14%,2C due to a sample failing during demoulding, 9 samples remained usable. The average Young's moduli are shown in Table 2.4 and a stress-strain curve for each composition can be seen in Figure 2.4. Data exceeds the 2.0 strain mark, however data were considered linear form this point. Therefore, no Young's moduli for a strain > 2.0 was calculated.

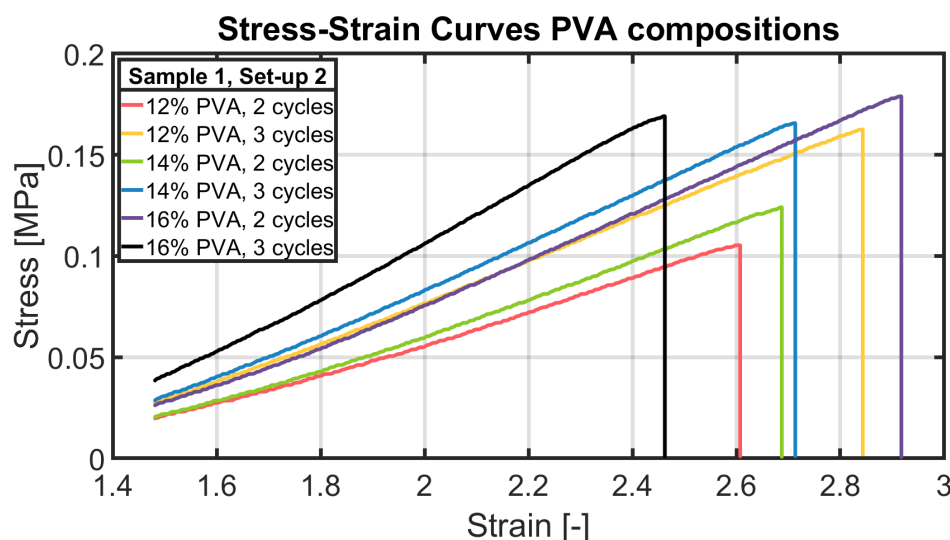
Both Table 2.4 and Figure 2.4 show a clear difference between the compositions of PVA-hydrogel. An increase in %-PVA with same number of cycles or increase in number of cycles with same %-PVA, both result in higher Young's moduli. The difference between 2 and 3 freeze-thaw cycles results in a larger difference in Young's moduli compared to a different amount of PVA used in the manufacturing process.

Table 2.4: Results Tensile test 2, comparison of the Young's moduli of 6 different compositions of PVA-hydrogel.

PVA [%]	Cycli [-]	N [-]	M1.5 [MPa]	SD [-]	M1.6 [MPa]	SD [-]	M1.7 [MPa]	SD [-]	M1.8 [MPa]	SD [-]	M1.9 [MPa]	SD [-]	M2.0 [MPa]	SD [-]
12	2	10	0.064	0.006	0.064	0.002	0.065	0.002	0.072	0.002	0.075	0.002	0.080	0.002
12	3	10	0.090	0.003	0.092	0.004	0.093	0.002	0.099	0.003	0.101	0.004	0.105	0.004
14	2	10	0.066	0.003	0.069	0.003	0.075	0.004	0.080	0.004	0.082	0.006	0.089	0.005
14	3	9	0.094	0.007	0.098	0.003	0.100	0.003	0.108	0.004	0.113	0.005	0.114	0.004
16	2	10	0.083	0.002	0.084	0.005	0.091	0.003	0.098	0.005	0.104	0.002	0.109	0.004
16	3	10	0.118	0.006	0.117	0.007	0.127	0.007	0.134	0.008	0.136	0.008	0.141	0.008

The Young's modulus is calculated for every 0.1 of strain (1.5 - 2.0), over  $\pm 0.05$  strain.

N: number of samples tested, MX.X: Young's modulus at X.X of strain, SD: standard deviation.



Shown sample was chosen on being closest to the mean result for all found Young's moduli.

Figure 2.4: Stress-strain plots of the mean sample of each PVA-hydrogel composition.

### 2.4.2. Different tensile samples

Tensile test 4 and 5 were performed to compare the influence of the different sample types (1, 2, 3) on the calculated Young's moduli. Similar to the previous tests, Figure 2.5 does show the graphs surpassing the 100% strain mark, however data were considered linear from this point and therefore, no Young's moduli for a strain > 100% was calculated. This is confirmed by the data from Table 2.5.

All three sample show some non-linear mechanical behaviour especially for the lower amounts of strain. Sample type 1 differs a lot from the other two samples. This is probably due to the force-stress conversion which is based on the cross-section of both strands instead of the single strand with type 2 and 3.

Table 2.5: Results Tensile test 4 and 5, comparison of the Young's moduli of 6 different tensile types .

Sample	M1.1 [MPa]	SD [-]	M1.2 [MPa]	SD [-]	M1.3 [MPa]	SD [-]	M1.4 [MPa]	SD [-]	M1.5 [MPa]	SD [-]
Type 1	0.029	0.001	0.034	0.004	0.035	0.003	0.038	0.003	0.049	0.003
Type 2	0.084	0.009	0.070	0.007	0.099	0.022	0.110	0.011	0.120	0.008
Type 3	0.053	0.007	0.047	0.008	0.050	0.004	0.071	0.011	0.076	0.008

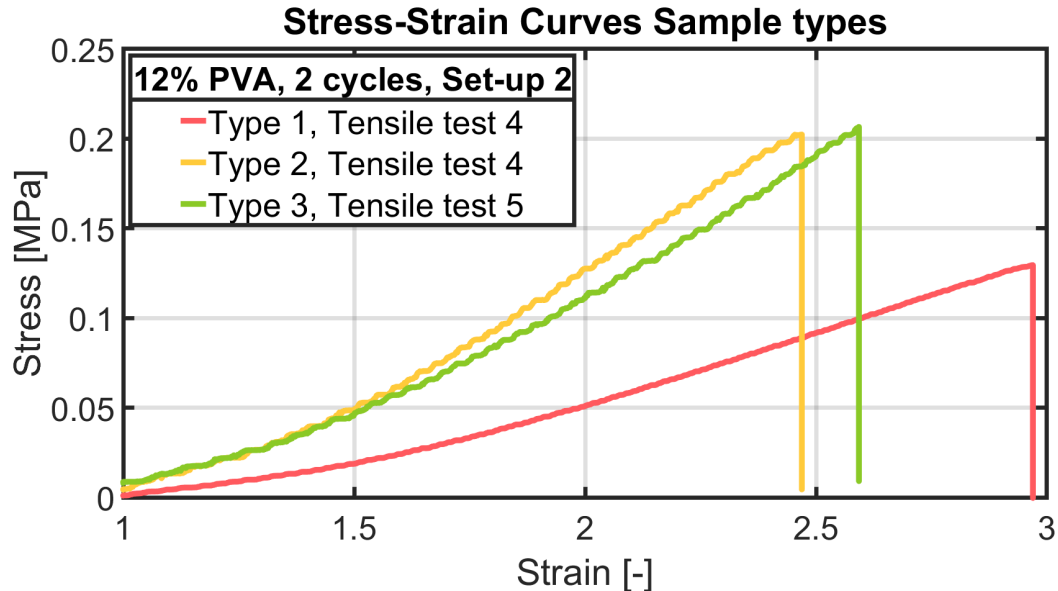
  

Sample	M1.6 [MPa]	SD [-]	M1.7 [MPa]	SD [-]	M1.8 [MPa]	SD [-]	M1.9 [MPa]	SD [-]	M2.0 [MPa]	SD [-]
Type 1	0.056	0.005	0.061	0.002	0.067	0.004	0.072	0.004	0.072	0.004
Type 2	0.138	0.017	0.156	0.009	0.160	0.012	0.166	0.008	0.162	0.009
Type 3	0.082	0.007	0.088	0.014	0.098	0.011	0.099	0.009	0.102	0.012

The Young's modulus is calculated for every 0.1 of strain (1.5 - 2.0), over  $\pm 0.05$  strain.

N: number of samples tested, MX.X: Young's modulus at X.X of strain, SD: standard deviation.

Each batch is 12% PVA, 2 cycles PVA-hydrogel, and consists of 10 individual samples.



Shown sample was chosen on being closest to the mean result for all found Young's moduli.

Figure 2.5: Stress-strain plots of the mean sample of each sample type.

### 2.4.3. Comparing different test set-ups

Tensile test 6 and 7 were both performed with the same set of samples, sample 1-5 were only tested using set-up 2, all samples were used for the test with set-up 3. Looking at the resulting plot showing the individual stress-strain curves. A difference between the samples already used and the unused samples could be easily seen in Figure 2.7. Therefore for the results in Table 2.6 only sample 6-10 were used for the average Young's moduli calculations, since these samples were not used in prior testing.

These results compared set-up 2 with set-up 3. The main difference between the set-ups is the type of fixation: rod fixation vs fully form-fitted fixation of the ends of the sample. From the table (2.6) and figure (2.6), samples tested using set-up 3 result in higher Young's moduli compared to set-up 2.

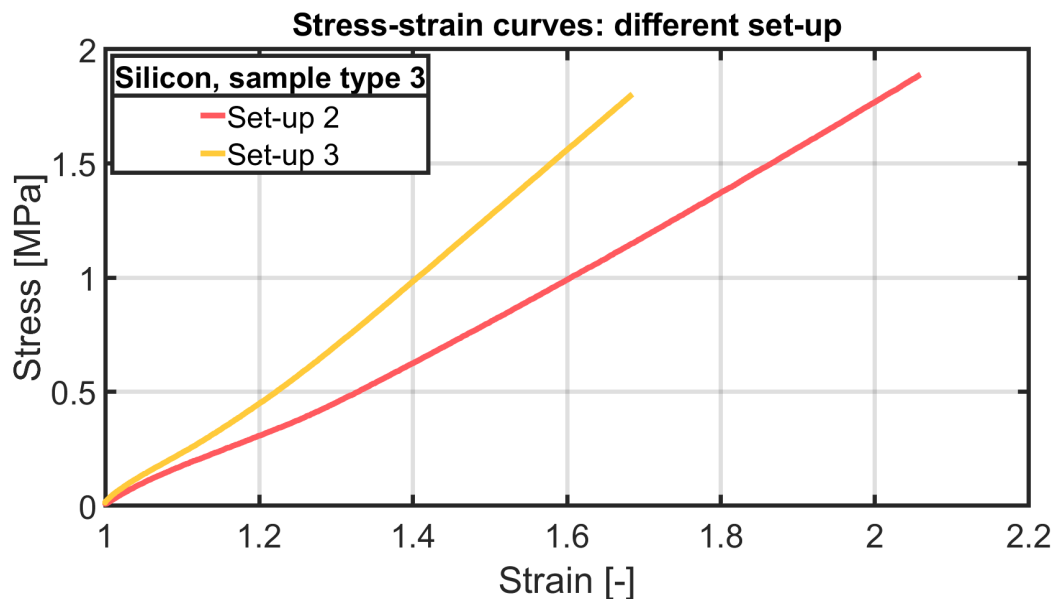
Table 2.6: Comparison between average Young's moduli using set-up 2 and 3, for both silicone rubber and PA-hydrogel.

PVA	M1.1 [MPa]	SD [-]	M1.2 [MPa]	SD [-]	M1.3 [MPa]	SD [-]	M1.4 [MPa]	SD [-]	M1.5 [MPa]	SD [-]	M1.6 [MPa]	SD [-]
Set-up 2	0.053	0.007	0.047	0.008	0.050	0.004	0.071	0.011	0.076	0.008	0.082	0.007
Set-up 3	0.102	0.008	0.130	0.011	0.126	0.009	0.134	0.015	0.131	0.011	0.148	0.020

Silicone	M1.1 [MPa]	SD [-]	M1.2 [MPa]	SD [-]	M1.3 [MPa]	SD [-]	M1.4 [MPa]	SD [-]	M1.5 [MPa]	SD [-]	M1.6 [MPa]	SD [-]
Set-up 2	1.430	0.135	1.348	0.239	1.487	0.330	1.612	0.353	1.691	0.313	1.766	0.229
Set-up 3	1.888	0.317	2.262	0.566	2.571	0.635	2.719	0.521	2.857	0.277	3.086	0.283

The Young's modulus is calculated for every 0.1 of strain (1.1 - 1.6), over  $\pm 0.05$  strain.



Shown sample was chosen on being closest to the mean result for all found Young's moduli.

Figure 2.6: Comparison of set-up 2 and set-up 3, both set-ups were used with silicone samples.

#### 2.4.4. Plastic deformation of samples

During tensile test 7, a difference between the samples already used during a tensile test and samples which were not tested before was seen, as shown in Figure 2.7. Sample 1 and 2 were used multiple times prior to the actual test to determine the maximum stroke length for the linear stage to ensure the stage not being overloaded during testing. These samples are shown as black dotted lines in Figure 2.7. Sample 3-5 were previously tested as well but only a single time, these are the full lines in the figure. Sample 6-10, show a clearly different mechanical behaviour compared to the previous five samples, except for sample 8. Which shows a curve very similar to samples 3-5 which were tested prior to tensile test 7, an explanation for this could be that the sample was tested in a practice run prior to the numbering of the samples.

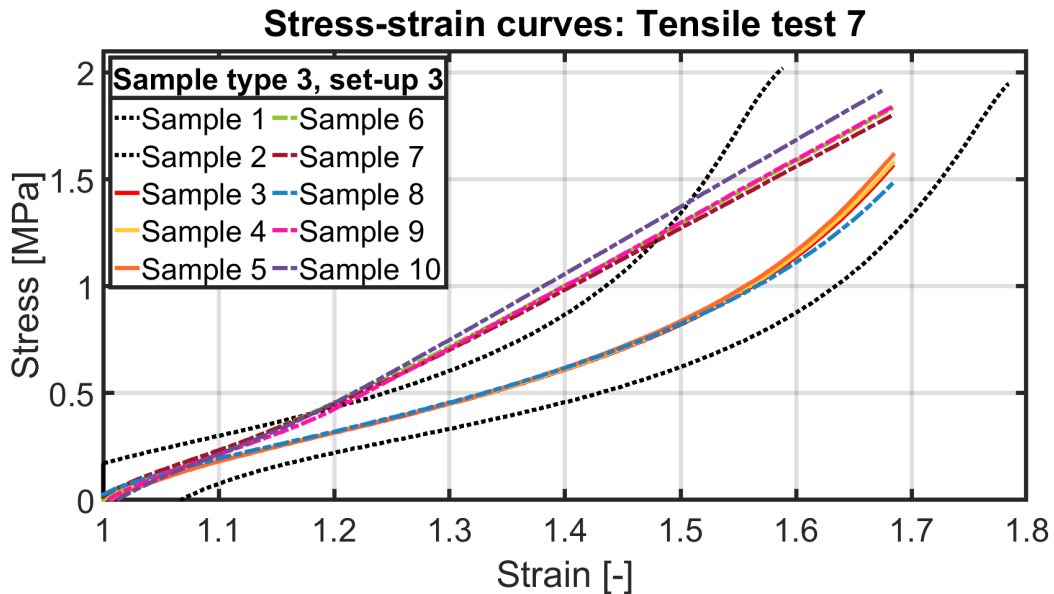


Figure 2.7: Stress-strain curves of tensile test 7, showing the influence of prior testing on tensile samples.

Since both test 6 and 7 were performed on the same day of testing, this difference between samples could be of a temporarily nature. To check whether this was a temporary or permanent effect, all samples from tensile test 9 were tested again one week after the previous test. The average result comparing the sample 1-5 from test 7 and sample 1-10 from test 9 are shown in Table 2.7. The difference between the two tests is minimal, therefore the effect of prior testing was seen as a permanent effect.

Sample 1 and 2, which had been stretched multiple times, show no different behaviour compared to other samples, when looking at the stress-strain curves of tensile test 9 (Appendixsection A.4). No clear difference was noticed between samples which were tested more than once compared to only a single prior test.

Table 2.7: Comparison of tensile test 7 and 9, comparing the influence of prior testing.

Tensile test	M1.1	SD	M1.2	SD	M1.3	SD	M1.4	SD	M1.5	SD	M1.6	SD
	[MPa]	[-]										
7, sample 1-5	1.514	0.303	1.310	0.103	1.518	0.342	2.063	0.784	3.276	1.923	3.947	0.429
9, sample 1-10	1.535	0.158	1.348	0.108	1.515	0.112	1.907	0.141	2.561	0.266	3.838	0.544

The Young's modulus is calculated for every 0.1 of strain (1.1 - 1.6), over  $\pm 0.05$  strain.

### 2.4.5. Pre-conditioning

Pre-conditioning of HAVW tissue was performed in the study of Lopez et al. [13]. Since a permanent effect of prior testing was already observed in this study, a tensile test to experiment with the influence of pre-conditioning was performed. This test was performed using a new batch of silicone rubber samples. Samples were divided into three groups: no pre-conditioning, single time pre-straining of 0.175, and triple pre-straining of 0.175, with the first group consisting of four samples and the other groups of three samples. Figure 2.8 shows the stress-strain curve of last sample group (triple pre-straining), only the first pre-straining appears different from the full strain.

The average results from Table 2.8 were calculated with the data of the full strain movement. The samples without pre-straining and the 3x pre-straining show very similar results for M1.3-1.6, while the 1x pre-straining samples appear to have some slightly higher Young's moduli compared to the other samples. Data from the table on the second and third pre-straining confirms that these two movements do not differ from each other in terms of Young's modulus.

Since the data shows no apparent trend between number of times of pre-straining and the resulting Young's moduli. This could be due to the amount of strain (0.175) already causing plastic deformation, since any pre-straining after the first one is similar to the full strain.

Table 2.8: Average Young's moduli for samples with different amounts of pre-conditioning.

Sample	M1.1 [MPa]	SD [-]	M1.2 [MPa]	SD [-]	M1.3 [MPa]	SD [-]	M1.4 [MPa]	SD [-]	M1.5 [MPa]	SD [-]	M1.6 [MPa]	SD [-]
No pre-straining	1.784	0.029	2.167	0.094	2.631	0.037	2.846	0.008	2.911	0.046	2.881	0.075
1x pre-straining	2.116	0.021	2.394	0.018	2.857	0.070	3.011	0.079	3.030	0.095	3.078	0.057
3x pre-straining	1.955	0.009	2.274	0.088	2.644	0.128	2.832	0.035	2.858	0.044	2.878	0.021
	1st	SD	2nd	SD	3rd	SD						
1x pre-straining	2.071	0.034	-	-	-	-						
3x pre-straining	2.038	0.169	2.202	0.045	2.201	0.048						

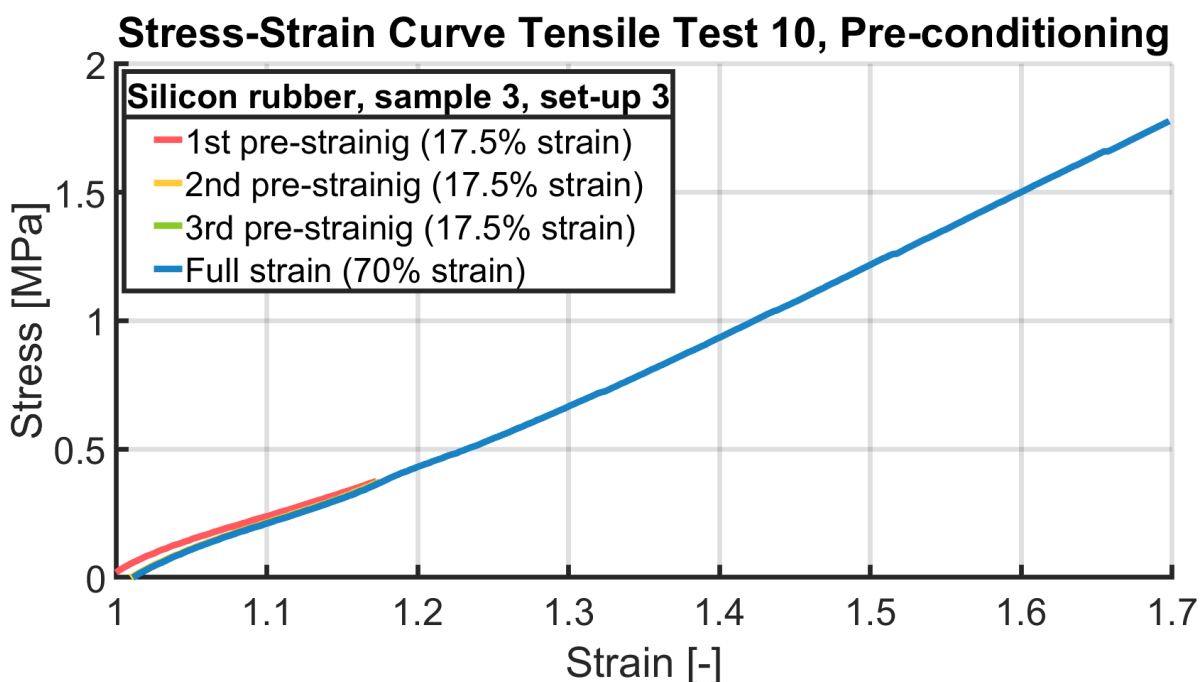
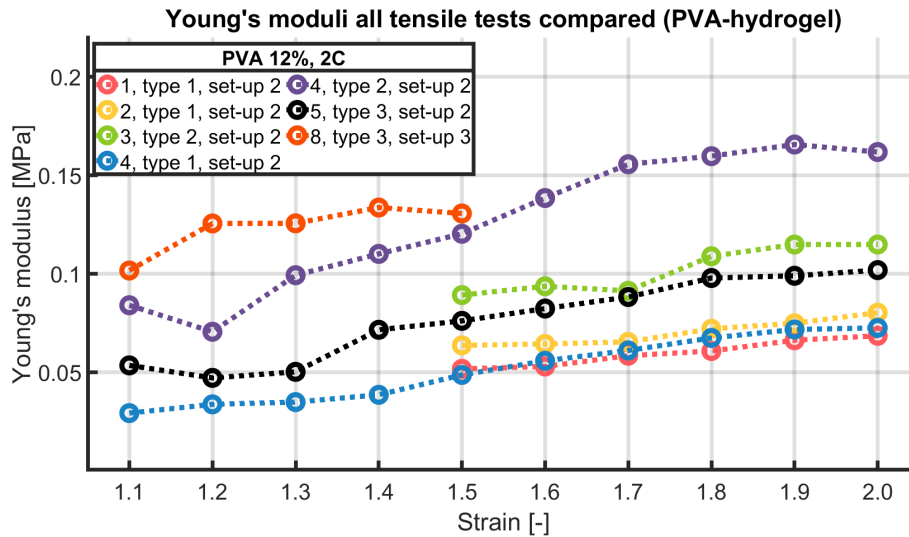


Figure 2.8: Stress-strain curve for a sample with 3x pre-straining prior to the full strain-movement as pre-conditioning.

## 2.5. Discussion

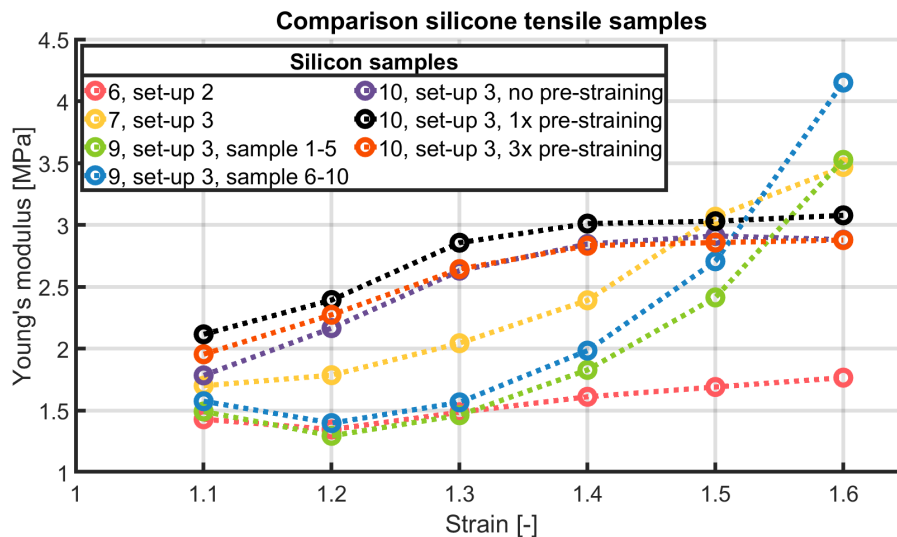
Now that all results of the different tests have been shown, the results can be compared to the data from literature. Furthermore, the choice made during the process of tensile testing will be discussed, and future testing is discussed in this section.

The found Young's moduli resulting from all different sample types and set-ups, for PVA-hydrogel and silicone rubber are shown in Figure 2.9 and 2.10. The Young's moduli calculated for PVA-hydrogel were a lot less high compared to those for silicone rubber, <0.2 MPa and >4 MPa respectively.



Dotted lines are a linear interpolation between point, and are not measured.

Figure 2.9: Range of Young's moduli found for PVA-hydrogel, comparing different sample types and set-ups.



Dotted lines are a linear interpolation between point, and are not measured.

Figure 2.10: Range of Young's moduli found for silicone rubber, comparing different sample types and set-ups.

### 2.5.1. Comparison with literature

The Young's moduli found during this study have been presented in the previous two figures (2.9, 2.10). Samples tested in this study did not meet the range of 6.7 - 14.4 MPa for the Young's modulus for HAVW found in literature. Using samples with a smaller cross-section could increase the amount of strain without exceeding the limitations of the stage. When looking at the moduli calculated in tensile test 9, show still increasing moduli at the 1.6 strain-point. Extrapolation of this data suggest that the moduli will eventually be within the range of 6.7 - 14.4 MPa. However, this will require larger amounts of strain compared to the amount of strain achieved in the tensile tests.

Since the Young's modulus is only a single value representing the slope of a curve, using this value to represent the complete tensile behaviour of the material will only be a good approximation when the material exhibits linear behaviour or when load exerted to the sample is within the linear range. Based only on the reported Young's moduli the tensile behaviour of HAVW cannot be determined, therefore additional data were required to determine whether the used data from literature can accurately represent the tensile behaviour.

Only the study of Martins et al. [1] and Lopez et al. [13], include graphs to report the results of tensile testing other than the found moduli, from the studies used for the Young's modulus range. Figure 2.11 shows the stress-strain curve for the different types of tissue compared during the study of Martins et al., the yellow line projected in the figure is the result of tensile test 10 (1x pre-straining). A clear difference between the data from the study of Martins et al. compared to the samples tested during this study, is the non-linear behaviour of HAVW-tissue mainly for low strain. This non-linear behaviour could explain the difference in Young's moduli between actual HAVW-tissue and the PVA-hydrogel and silicone rubber samples.

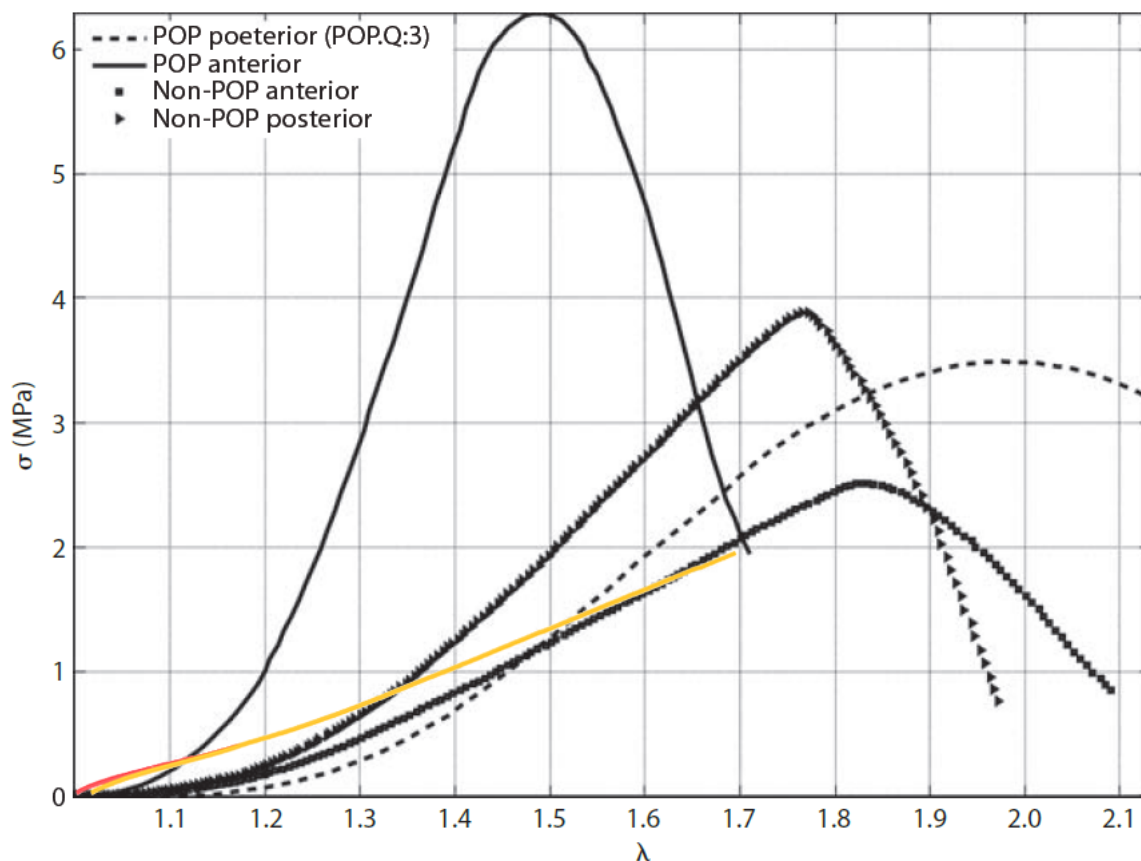


Figure 2.11: Stress-strain curve (Tensile test 10, 1x pre-straining) projected onto the graph from the study of Martins et al. [1]

When comparing the curves from Figure 2.11, the Non-POP anterior line (lowest peak in the figure) and the full strain curve between 1.5 and 1.7 of strain, you can observe that the amount of stress is quite similar. This would suggest that silicone rubber could be used to mimic the bio-mechanical properties for HAVW-tissue according to the data from the study of Martins et al., but only for a certain window of strain.

The amounts of stress measured with the PVA-hydrogel samples is much lower, 0.2MPa of stress occurs at a strain of 2.5 for the PVA-hydrogel while this already occurs around a strain of 0.2 for the HAVW-tissue. In order for selecting a material to be used in developing a phantom, the conditions (amount of strain expected) during testing will have a large influence on which mechanical behaviour the phantom should exhibit.

Another study which was not originally included, due to not reporting a single value for the Young's modulus for HAVW-tissue, was the study of Chantereau et al. [2]. This study compared different organs in the pelvic region, and divided the mechanical behaviour into two parts. To describe these two parts, two directional coefficients were calculated for each type of tissue. Similar to the previous study the results of the study are compared by projecting the results of tensile test 10 (1x pre-straining) onto the graph (2.120 showing the results of the study of Chantereau et al.. The result of tensile test 10 is located between the two lines representing the different type of vaginal tissue (young and old) compared in the study.

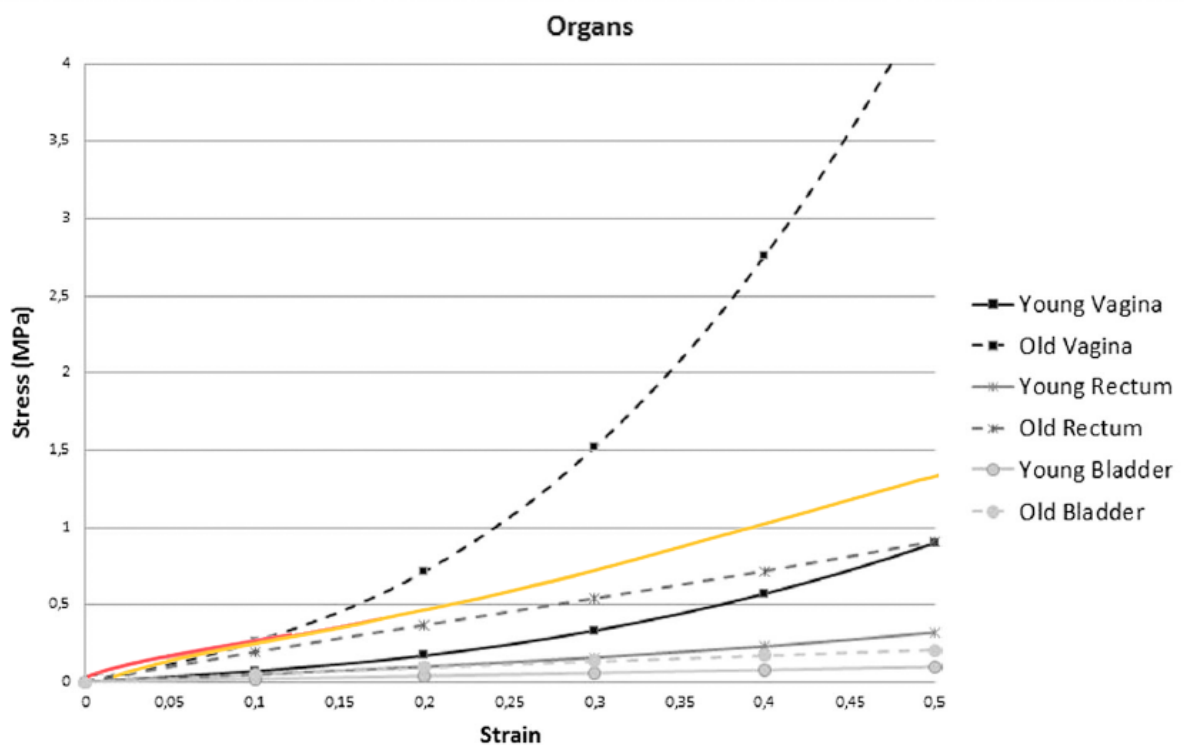


Figure 2.12: Stress-strain curve (Tensile test 10, 1x pre-straining) projected onto the graph from the study of Chantereau et al. [2]

### 2.5.2. Set-up

Since a large part of this study revolves around determining the mechanical properties of samples, the set-up used during this study plays a vital role in the gathering of data, therefore the used set-up and choices in regard to this set-up are discussed. Firstly, the linear stage has a large impact on the performance of the entire set-up. This linear stage is not designed for performing tensile testing but for needle puncture testing. The first limitation of this set-up is the minimal movement speed of the stage, the current set-up was capable of movements down to tenths of mm/s, while set-ups developed for tensile testing can perform testing at tenths of mm/min. Slower speeds could allow the materials to adjust to the imposed strain, increase the amount of strain prior to failure by rupture.

The tensile load cell used during testing was selected prior to testing. The sensor was selected with a large safety margin to prevent overloading the sensor. The limited pulling force of the linear stage was unknown prior to the experiment, otherwise the sensor could have been picked with lower force threshold which would probably increase the precision of the sensor. Step size of the load cell in combination with the signal conditioner was 0.005V or 0.13N, which results in a precision of 0.065N. This step size was monitored prior to the smoothing of the data. This precision is probably enough when performing tensile tests using silicone rubber samples, however for PVA-hydrogel samples which can already fail below 3N this precision might not be enough.

Testing with silicone samples was non-destructive due to high rupture toughness of the material and the limitations of the linear stage. The stage would stop moving or be pulled back a few centimeters when surpassing forces above 60N. To prevent this from happening, a maximum stroke was determined for each test using silicone samples. This value was determined by running the test multiple times with an increasing stroke. Since the samples were not destructed during testing, the samples were numbered to be differentiated for future tests.

### 2.5.3. Sample types

During testing three different types of samples have been tested, the reason for this different sample types is further elaborated.

#### Type 1

This sample was replaced because the sample tended to fail almost constantly (>95%, N=114) at either the upper or lower contact point between the sample and the fixation rods, see Figure 2.13. This resulted in a rather difficult failure mechanism, and the measured force to stress conversion (two parallel strands) was considered to be incorrect. Data collected using this type of sample however are used in this study, but are only compared to measurements obtained with the same type of sample.

#### Type 2

The second sample was designed to eliminate the chance of failure at the contact surface between the fixation rods and the sample. The thickness of the material is increased at both end of the sample, the thin strip in the middle is 3mm wide the material surrounding the opening is 5mm wide. The design resulted not in full elimination of failure at the fixation ends but reduced the chance (30%, N=20). However, all samples that did not fail at the contact surface did fail close to neck (transition area between the thick and thin part of the sample). Figure 2.14 shows the failure point of 10 samples after tensile testing.

#### Type 3

To further eliminate the failure at the contact surface, the thickness of the narrow part was decreased from 5mm to 3 mm. The thickness of the sample surrounding the fixation points was increased from 5mm to 9mm, and the transition in the narrowing part of the sample was made more gradual. Unfortunately this did not have the desired effect as can be seen in Figure 2.15 which shows the failure point of 10 samples after tensile testing. Since this sample type was also unsuccessful in eliminating the failure of sample at the fixation ends of the sample, a new set-up (set-up 3) was developed instead of developing yet another tensile sample.



Figure 2.13: Failure point of type 1 samples



Figure 2.14: Failure point of type 2 samples



Figure 2.15: Failure point of type 3 samples

#### **2.5.4. Future testing**

A wide range of tests have already been performed to measure the influence of multiple variables on the stress-strain behaviour of PVA-hydrogel and silicone rubber samples. Future testing which could prove useful for future research would include additional testing on the influence of pre-conditioning for silicone samples, by altering/varying the amount of pre-straining instead of keeping this constant. Pre-conditioning of PVA-hydrogel samples has not yet been performed, both these experiments would provide crucial information on the re-usability of any developed phantom. Data on the yield point of the materials would also determine the re-usability of a phantom, tensile test 9 has already confirmed plastic deformation occurring below 70% strain.

### **2.6. Conclusion**

The selected range (6.7 - 14.4 MPa) for the Young's modulus at the beginning of this chapter was not reached during this study. The Young's moduli found for silicone rubber (highest results >4MPa) were closer to the values reported in literature, compared to PVA-hydrogel (highest results <0.2MPa). Comparing the results visually to the graphs of other studies, did show the silicone rubber samples to match the bio-mechanical behaviour of HAVW-tissue.

During testing both materials (PVA-hydrogel and silicone rubber) exhibit a more linear behaviour compared to stress-strain curves of HAVW-tissue. This suggests that a material selected for the production of the phantom will only mimic the bio-mechanical properties of the HAVW-tissue for a window of strain instead of the full range.

# 3

## Indentation testing

The use of mechanical testing often requires destructive testing or results in plastic deformation of the tested material. Therefore, this method of testing is not suitable to validate the mechanical properties of a produced phantom, since the phantom will no longer be usable after testing. An alternative method was required for non-destructive mechanical testing without the need for a prescribed shape. The method selected for this purpose is indentation testing.

### 3.1. Methods

All samples were made using the same mould, creating a conical frustum shape. The samples were removed from the fridge one hour prior to the experiment to adjust their temperature to the surroundings before testing occurred. The samples were taken from their plastic containers with water, half an hour prior to the experiment and patted dry. This was done to reduce the risk of slippage of the instrument during the experiment.

The instrument used in the experiments with PVA, was a Shore Hardness tester, HT 6510-00 (Dalian Teren Instruments Co., Ltd, Dalian, China). For experiments with silicon rubber, the HT 6510-A (Dalian Teren Instruments Co., Ltd, Dalian, China) was used. Difference between the two instruments is the scale of hardness used, the 6510-00 uses the Shore-00 scale which is used for gels, sponges and very soft types of rubber and the 6510-A uses the Shore-A scale which can be used for different type of rubber varying from soft to semi-hard. Both instruments use impression depth to determine the hardness of the material it contacts. Both devices were calibrated prior to testing (both 0- and max-load calibration) following the instructions. Mean, average and standard deviation calculations were performed using Excel 2016 (Microsoft Corporation, Redmond, Washington, USA)

The order of testing was randomized prior to the experiment. Each sample was tested 5 times, consisting of an average-value measurement which was performed by 9 individual measurements following the pattern shown in Figure 3.1. Individual measurements were not recorded, but were monitored to ensure proper testing. Starting a new measurement too early resulted in a negative value, if this happened the complete average-value measurement was started over.

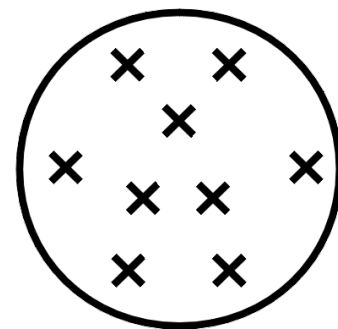


Figure 3.1: Pattern of individual measurements for an average-value measurement



Figure 3.2: Indentation test

### 3.1.1. Indentation test 1

The first experiment consisted of 18 PVA-hydrogel samples. These samples were made in six different batches using a different %-PVA during manufacturing (6%, 8%, 10%, 12%, 14%, or 16%, 3 samples each). The 3 samples from each batch differed in number of freeze-thaw cycles (2, 3, or 4). All samples were produced using the standard procedure described in Appendix section C.1.

### 3.1.2. Indentation test 2

The second experiment was performed to determine the influence of the storage time on the hardness of the stored PVA-hydrogel sample. For this test two samples were used, these sample were tested prior to submersion, and after submersion for: 24 hours, 48 hours, 72 hours, 1 week, 2 weeks and 3 weeks.

### 3.1.3. Indentation test 3

The third experiment was performed using silicon rubber samples. Testing included storage of the sample over a period of three weeks (similar to the PVA-hydrogel samples in tensile test 2). The influence of silicone thinner, which was used during the manufacturing of the phantom. Finally, the influence of storage in water, during the dissolving of the PVA-insert, for the phantom production process was tested.

## 3.2. Results

The results of the indentation test 1 are presented in Figure 3.3. The results for the sample (6%, 2C) are not displayed due to the sample sustaining permanent damage from the instrument during the indentation test. The sample was not stiff enough to provide proper resistance for the test to be performed without damaging the sample. The graph shows clear differences between samples with the same number of freeze-thaw cycles but a different amount of PVA used during manufacturing. The difference between samples with the same amount of PVA used during manufacturing but different number of freeze-thaw cycles, is shown in graphs which can be found in Appendix section B.1. The difference between 2 and 3 cycles have a greater impact compared to the difference between 3 and 4 cycles, this is clearly visible for sample 8, 10, 12, and 14%.

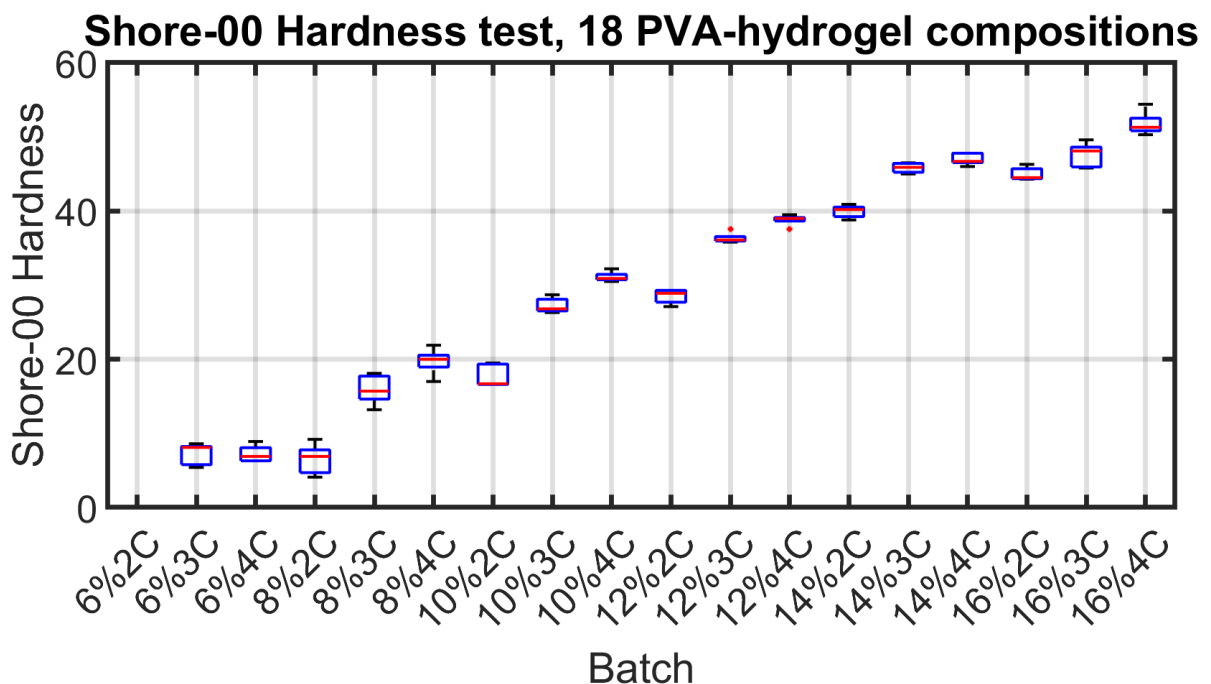
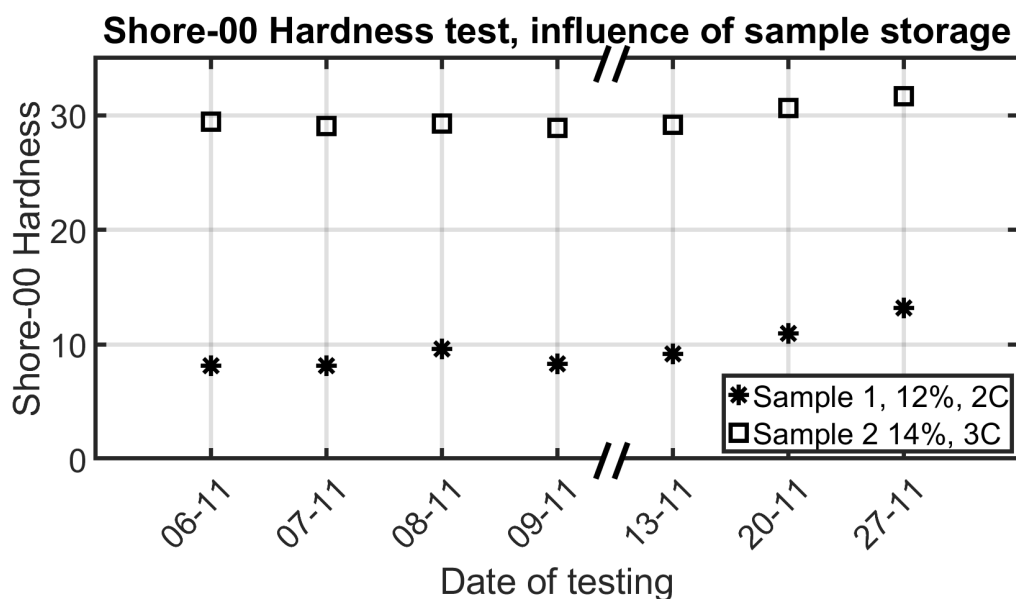


Figure 3.3: Hardness results from indentation test 1. Each box represents 5 average-measurements which consist of 9 individual measurement.

### 3.2.1. Tensile test 2

The progress of the hardness of two samples was monitored over a period of 3 weeks, with intermediate measurements. The results of these measurements are shown in Figure 3.4, the individual measurements can be found in section B.2.



Break in axis, switch from days to weeks.

Figure 3.4: Results indentation test 2, testing the influence of sample storage over time.

### 3.2.2. Indentation test 3

This test was performed with silicone rubber samples. Testing included storage of the sample over a period of three weeks (similar to the PVA-hydrogel samples in tensile test 2). The influence of silicone thinner, which was used during the manufacturing of the phantom. Finally, the influence of storage in water, during the dissolving of the PVA-insert, for the phantom production process was tested. The results are presented in the aforementioned order in Table 3.1.

Table 3.1: Results of indentation test 3, comparing different criteria on their influence on silicone rubber samples.

	M1	M2	M3	M4	M5	Mean	SD
Sample 1, 04-Nov	39.5	38.7	38.7	38.7	38.8	38.9	0.3
Sample 1, 25-Nov	38.8	37.8	38.8	39.4	39.3	38.8	0.6
Sample 2, 04-Nov	37.0	38.0	36.8	37.1	36.9	37.2	0.5
Sample 2, 25-Nov	36.9	35.6	34.7	37.0	37.3	36.3	1.1
Normal	38.2	40.7	40.1	39.7	40.6	39.9	1.0
Thinner	27.0	26.3	27.6	27.3	26.5	26.9	0.5
Phantom VW, 04-Nov	27.8	27.4	27.6	27.5	27.2	27.5	0.2
Phantom VW, 25-Nov	28.4	28.4	27.6	27.6	26.9	27.8	0.6
Phantom ST, 04-Nov	12.7	11.6	11.8	11.8	11.4	11.9	0.5
Phantom ST, 25-Nov	13.5	14.0	13.5	13.8	13.3	13.6	0.3

### 3.3. Discussion

Indentation testing as a method to verify the mechanical properties in a non-destructive method was tested. Different compositions of PVA-hydrogel have been compared, resulting in a range from 6.5 - 51.8 on the Shore-00 scale. Comparing these results with the results of tensile test 2, in which these compositions were tested as well, showed similar trends in the data when comparing the different composition against each other. Proving the method as viable alternative for tensile testing.

When testing PVA-hydrogel samples of a period of three weeks, while the samples were stored submerged in water, showed an increase in hardness of the samples over time. This increase could likely be explained by the physical changes of samples monitored over time. After the samples are manufactured, initially the samples have a tendency to swell, later this swelling is reversed and shrinkage of the samples takes place. This swelling and shrinkage will probably be the result of the amount of water absorbed. This result does affect the shelf life on a produced phantom, since the mechanical changes over time will influence the testing performed with the phantom.

The samples were intended to be placed in a 3D-printed ring to hold the sample in place, as can be seen in Figure 3.5. However, the samples with a high quantity of PVA resulted having a very uneven surface which was considered unusable for the indentation test. The tip of the instrument is small enough to fit in between the ridges present at the surface of the sample, which could result in discrepancies between different measurement points along the surface of the sample. Therefore, the samples were flipped upside down to use the smooth surface instead. This resulted in the ring no longer being suitable for the fixation of the samples. However, fixation proved unnecessary since the sample did not have the tendency to move during testing.

All samples created for the tensile tests were manufactured using the left-over material, resulting in different amounts of material used for the production of the indentation samples. Higher amounts of material used for producing a sample, results in a thicker sample. Any influence of the thickness on the results of the indentation test was not tested, thicknesses of the individual samples are recorded and can be found in the tables in Appendix B. To eliminate this difference in thickness for future testing, the use of a closed mould is recommended.

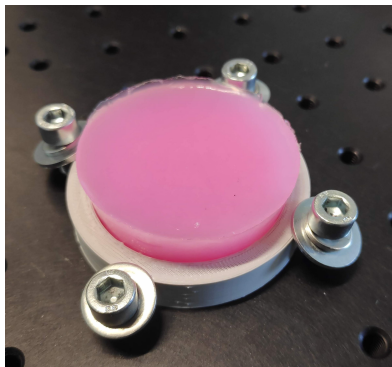


Figure 3.5: Designed fixation cup for indentation testing.



Figure 3.6: Rough surface of a PVA-hydrogel sample, this requires the samples to be tested upside-down



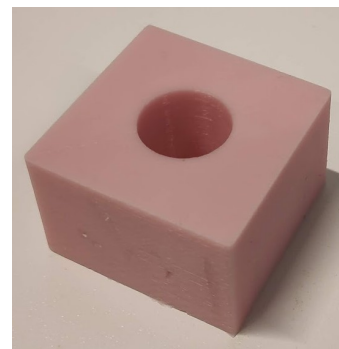
Figure 3.7: Tip of the shore hardness tester.

# 4

## Visibility

In brachytherapy visualization of target structures is performed either by CT or MR-imaging. In the project developing the customized applicators, the focus is on MR-imaging. In order for the phantom to be used without the need for a different procedure or adjusted settings for the MR-scanner, the phantom should have proper contrast compared to other materials or instrumentation used during procedures for brachytherapy.

Testing was performed at Erasmus Medical Centre. The test consisted of multiple samples and phantoms being placed inside a MRI-scanner. The samples contained a cavity which could be filled with ultrasound gel or be left empty, the dimensions of the cavity were known. Intensity measurements were performed using these two structures (cavity and the surrounding sample) to quantify the differences between different materials.



The sample in the image is manufactured from silicon rubber (Smooth-Sil 940).

Figure 4.1: Shape of the samples used during the MRI-experiment.

### 4.1. Samples

The samples were designed to have a very simple geometric shape, a cube with a cylindrical cavity in the top surface of the cube. Figure 4.1 shows one of the samples manufactured from silicon, the cavity on the top of the cube is empty. The samples were filled with ultrasound gel, to simulate the testing of filling the vaginal cavity with ultrasound gel in real patients, which is a procedure that is being developed at the Erasmus Medical Centre in order to properly visualize the vaginal cavity in patients.

During testing eight samples and two phantoms were compared on contrast in the MR-images. Four of the samples were manufactured of PVA-hydrogel, the remaining four samples from silicon rubber. One phantom was manufactured from PVA-hydrogel, the other from silicon rubber. Exact materials and manufacturing procedures can be found in Appendix C.

The PVA-samples had the following compositions:

- 14%, 3 cycles (two samples)
- 8%, 2 cycles (single samples)
- A sample with an inner layer of 14%, 3 cycles and a surrounding layer of 8%, 2 cycles.

The silicon-samples were manufactured as followed:

- Smooth-Sil 940 (two samples)
- Sorta clear 18 (single sample)
- A sample with an inner layer of Smooth-Sil 940 and a surrounding layer of Sort Clear 18.

## 4.2. Data acquisition and processing

Testing was performed using a Optima MR 450w 1.5T scanner [GE Healthcare, Chicago, USA] at the Erasmus Medical Center, which was controlled by a medical specialist. The samples and phantoms were placed on a MR-compatible tray. The second coil was placed above the tray, this is standard for the procedure normally used with brachytherapy patients. Additional information of the position of the samples and phantoms on the tray, can be found in Appendix D.

A total of 6 scans were made, the settings of these scans can be found in Appendix D. The slices of the different scans were visually inspected to determine which dataset would be used for the intensity measurements, a LavaFlex InPhase (TR: 6.7, TE: 3.3) image was selected to be used. This choice was based on the visual contrast observed.

Data processing was performed with the provided viewing software [GE Healthcare, Chicago, USA], a tool for intensity measurements was part of the viewing software. Measurements were done by dragging a circle to the area which needed to be measured. Each structure was measured using three individual measurements. The circle used for intensity measurements was kept the same size ( $95.8 \text{ mm}^2$ ) for most of the measurements. Only for the additional layer of two double layered samples and the VW-layer of both phantoms, smaller circles ( $33.2$  and  $5.8 \text{ mm}^2$  respectively) were used.

For each area (core, sample, phantom) three measurements were performed. The circles used for the measurements were attempted to be placed without overlap if possible and scattered around the area. In Figure 4.2 the MR-image used for measurements is shown with the three different sets of circles used for intensity measurements. The results on max, average and standard deviation of the intensity can be found in Table D.1 of Appendix D. These three average measurements are averaged again to a single value, to calculate the difference between the different structures present in the MR-image. The resulting differences are shown in Table 4.1.

## 4.3. Future testing

The difference between the different compositions of the same materials can be clearly seen by an untrained person, which was not expected prior to the experiment. These differences (between different compositions) are less distinct compared to the differences between silicon rubber/PVA-hydrogel and ultrasound gel/air, which was the expected result of the experiment. A material that was not included in this experiment but could be interesting for future testing, would be 3D-printed material representing the customized applicator. As tested in the study of Laan et al. [15].

Table 4.1: Differences in signal intensity between the different materials/compositions measured in the MR-image.

Combination	Difference
Silicon 940 - Air	177.8
Silicon 940 - UG	406.3
Silicon 18 - UG	337.9
Silicon 940 - Silicon 18	158.5
<b>Phantom</b>	
Silicon VW - UG	284.6
Silicon ST - UG	129.1
Silicon VW - Silicon ST	155.5
PVA 14%, 3C - Air	1585.7
PVA 14%, 3C - UG	667.1
PVA 8%, 2C - UG	287.0
PVA 14%, 3C - PVA 8%, 2C	283.6
<b>Phantom</b>	
PVA VW - UG	550.7
PVA ST - UG	496.6
PVA VW - PVA ST	54.1

UG: ultrasound gel

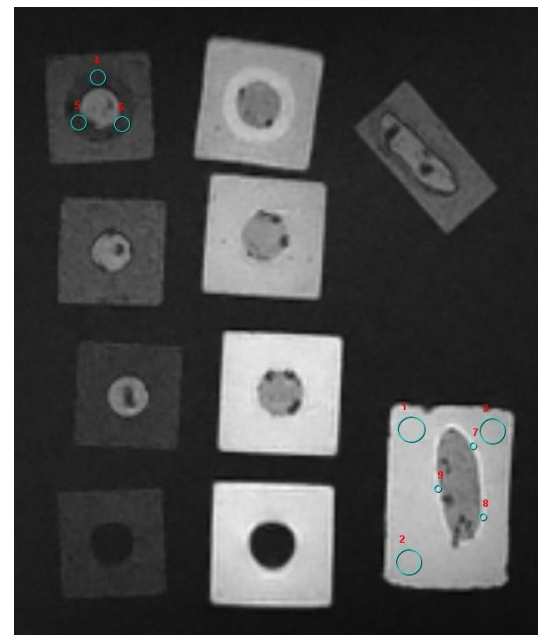


Figure 4.2: MR-image used for intensity calculations, the cyan circles mark the areas used for intensity measurements.

# 5

## Phantom production

In this chapter the process of producing a phantom is described and visualized. Both silicon rubber and PVA-hydrogel have been used to produce at least one phantom. The various moulds developed during this study can be found in section E.2 of Appendix F.

### 5.1. Digital design

During the design of the phantom, structure mimicking the the vaginal wall being anatomically correct was considered to be more important compared to the surrounding tissue being anatomically correct. Thus the phantom was designed to consists of hollow vaginal cavity, surrounded by a layer mimicking the vaginal wall, and the vaginal wall was covered by a layer mimicking surrounding tissue. These two layers needed to have different bio-mechanical properties.

In the study of Laan et al. the development of a customized needle applicator is described, in the process a 3D structure of the vaginal cavity is developed [15]. This process consists of delineation of the vaginal cavity in MR-images by a medical specialist, followed by concatenation of the segmented contours, and surface mesh modeling to create a 3D structure. The pathways added in the study of Laan et al. could be omitted from the 3D structure of the vaginal cavity.

The 3D model of Laan et al. does not contain a separate 3D structure of the vaginal wall. Creating this layer was required, since this structure is required for the development of the phantom. A 3D structure of this layer with a simplified shape was developed using the 3D structure of the vaginal cavity as a basis. This process was performed using Solidworks 2019 [Dassault Systèmes, Vélizy-Villacoublay, France]. The structure was obtained by scaling the 3D structure of the vaginal cavity up to an enlarged model. Non-uniform scaling was used to grow the structure an equal amount in all directions. The outer surface of the obtained structure representing the edge of the vaginal wall at the transition with the surrounding tissue. Using the cavity function form Solidworks the initial model can now be subtracted, leaving with a thin walled structure representing the vaginal wall.

The layer mimicking the surrounding tissue was developed as an uniform layer, the bio-mechanical properties of this layer remain constant. In order to simplify production and handling of the phantom the outer shape of this layer was chosen to be a rectangular block.

### 5.2. Production process

The production of a phantom starts with 3D-printing a water-solvable PVA insert, PVA-filament is commonly used as a support material. The insert has the shape of the vaginal cavity, and can be dissolved when the manufacturing process of the other layers of the phantom are completed. The main function of this layer is to provide support to layer mimicking the vaginal wall, and defining the shape of the cavity in the phantom.

This insert is 3D-printed in separate parts, as can be seen in Figure 5.1. This is done to eliminate the need for support material during printing, since the material used for printing is normally used as a support material and removal is done by dissolving the support material in water over time. Furthermore, in order for the insert to dissolve faster in water, a lower infill percentage was chosen, this choice limits the mechanical strength of the insert which increases the risk of fracturing if mechanical removal of a support material was chosen. The individual parts are joined using a pin-hole connection, in which the pin is a separate part and inserted in holes in both halves of the insert. The pin is fixated using super glue.

After the glue is cured, the insert is inserted into a mould, the space between the insert and the mould is equal to the 3D-modeled vaginal wall. The cylinder on top of the insert is used to fixate and center the insert inside the mould. This mould is 3D-printed of PLA, the mould consists of 4 separate parts to fit around the insert. Figure 5.2 shows the insert inside the mould, one part of the mould is removed. The four parts of the mould are connected using pin-hole connections. Additional fixation of the mould is done by an outer mould around the base of the mould, and a ring fixating the top of the mould. Both the outer mould and fixation ring use bolts to fixate the individual parts of the mould. Centering of the insert is done using four bolts at the top of the mould. The latest version of the mould has a small container on the top of each part of the mould, a sloping channel connects the container to the inside of the mould. These containers function as a filling reservoir for the mould, which is required due to the high viscosity of the silicon rubber. In Figure 5.3 the fully assembled mould is shown while being filled with silicon rubber to manufacture the layer of the vaginal wall.

After the curing of the silicon rubber or the completion of the freeze-thaw cycles for PVA-hydrogel, the insert surrounded by the vaginal wall is removed from the mould. Figure 5.4 shows the manufactured vaginal wall form silicon rubber. For the manufacturing of the layer mimicking the surrounding tissue, the insert is suspended in an acrylic container, as can be seen in Figure 5.5. After the manufacturing process of this layer is completed, the walls of the container can be disassembled. The insert can be dissolved, resulting in a completed phantom (Figure 5.6).



Figure 5.1: 3D-printed insert, in separate parts.



Figure 5.2: 3D-printed insert inside the mold for the vaginal wall.

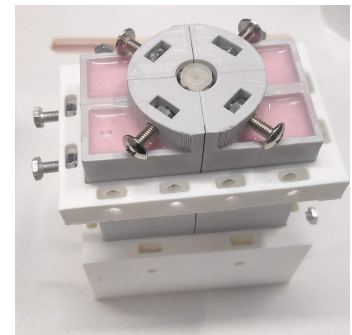


Figure 5.3: Mold for vaginal wall filled with silicon rubber.



Figure 5.4: Insert with vaginal wall after de-molding.



Figure 5.5: Insert with vaginal wall suspended inside mold for surrounding tissue.

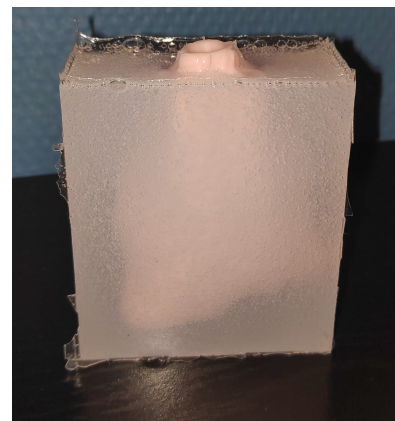


Figure 5.6: Complete phantom manufactured from silicon rubber.

# 6

## Phantom testing

The phantom which can be used to test methods for sealing the vaginal cavity, so that ultrasound gel can be used to fill the vaginal cavity improve the visibility of the vaginal cavity in MR-images. Visualisation of the vaginal cavity is an important step in the development of the customized applicators, since this will allow for a good adaptation of the applicator to the anatomy of the patient. For proper visualization of the vaginal cavity three challenges need to be solved: delineation, applicator fixation, vaginal packing. A possible solution to solve these challenges has already been developed at the Erasmus MC. The challenges and solution are further elaborated in this chapter.

### **Delineation**

The delineation on the vaginal cavity is needed to create a 3D-structure of this region, which is needed for the development of the personalized applicator. Improving contrast between the vaginal cavity and the vaginal wall, will result in improved ease and accuracy in the delineation process. By filling the vaginal cavity with ultrasound gel improved contrast was achieved, due to the high water content of the gel compared to the surrounding tissue. Swanick et al. have performed a study to compare different types of materials to be used as vaginal packing material during gynaecological brachytherapy, ultrasound gel proved to created the best contrast between the anatomy of the patient and the inserted applicator [21].

### **Applicator fixation**

Fixation of the applicator is essential for brachytherapy, the dose distribution calculations are based on the MR-images with the applicator in situ. Any shifts or movements of the applicator can result in over or under dosage of target or surrounding structures. To ensure the best possible fixation the customized applicator should follow the anatomy of the patient as close as possible. This requires also the shape and position of different organs inside the pelvic region to be similar as during the radiation procedure. By expanding the vaginal cavity during the MR-procedure a better fixation is created, since the vaginal wall will already be strained and thus deform less easily.

### **Vaginal packing**

The natural state of vaginal cavity is not similar to that during a brachytherapy procedure. In the natural state the vaginal cavity is unstrained which results in the anterior and posterior wall of the vagina folded inwards onto itself. During the brachytherapy procedure this is undesired, since this will result in increased exposure of surrounding tissue to radiation. To minimize the exposure of surrounding tissue the vaginal cavity needs to be maximally expanded (within the comfort of the patient), this is also done during normal brachytherapy procedure and is known as vaginal packing and often gauze is used. By expanding the vaginal cavity while the recording of the anatomy is performed, the customized applicator could accomplish the function of the vaginal packing material as well.

## Goal of the phantom testing

The procedure of filling the vaginal cavity with ultrasound gel, while MR-images are made, has already been performed at the Erasmus Medical Center. During the procedure some difficulties have surfaced during this initial test. The main difficulty found during experimental trails using expanding of the vaginal cavity using ultrasound gel, was the leakage of the ultrasound gel during the MR-procedure. During my internship at the Erasmus MC prior to this study, I have studied the problem and developed a few concepts which could resolve the leakage. Testing without the need for actual patients to compare the developed concept was preferred but required a phantom which could be used. Since a phantom was developed in this study the experiment can now be performed.

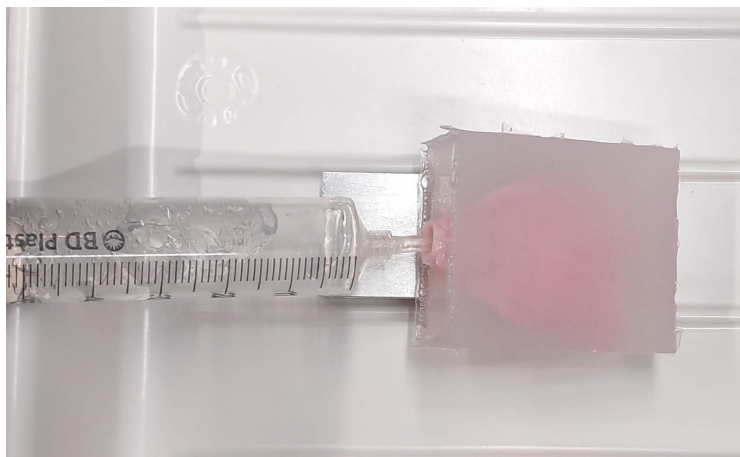
## 6.1. Methods

The set-up for this experiment consists of the developed phantoms (PVA-hydrogel and silicon rubber) being placed inside a container on a scale. The phantom is placed under a 20°-angle with the horizontal axis to match the anatomy of the patient. This angle was determined using the MR-images for the creation of the 3D-structure of the vaginal cavity, used in this study for the development of the phantom. The phantom is then filled with ultrasound gel until the gel starts to leak from the cavity of the phantom. Some overfilling is performed to ensure removal of any air pockets present inside the phantom. The set-up is left for 15 minutes, so any further leakage of ultrasound gel could occur. An example of this can be seen in Figure 6.1b. After 15 minutes, the catheter was clamped shut and any excess gel on the outside of the phantom was scraped off and placed in the container. The phantom was then removed from the scale and was weighted, using a different scale, to compare with the measurement performed prior to the experiment. The syringe used for the filling of the phantom was also measured after being filled with ultrasound gel and after the experiment to determine the amount of gel inserted. Figure 6.1a and 6.1b show the filling and over-filling during the pilot experiment.

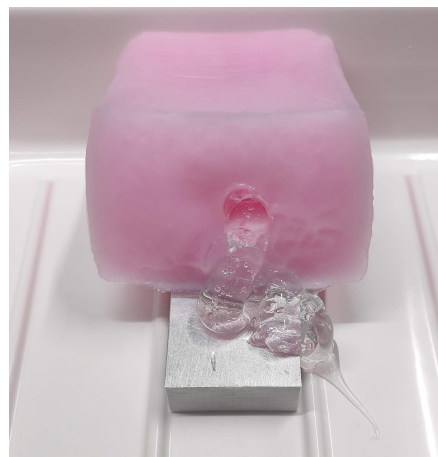
### 6.1.1. Instrumentation

The experiment was repeated using the different concepts. A pilot was performed prior to other tests to check the testing protocol. Equipment presented below were provided by the Erasmus Medical centre.

- The pilot was performed using a 60ml Plastipak syringe with Luer lock [BD, New Jersey, USA] with a 7cm rubber tubing attached ( $\varnothing$ 5mm, 1mm wall thickness).  
The ultrasound gel used was Aquasonic Clear [Parker Laboratories inc, New Jersey USA]. [22]
- Subsequent tests were performed using a 60ml Plastipak catheter tip syringe [BD, New Jersey, USA], and supragel ultrasound gel [LCH medical products, Paris, France]. [23]
- In the first experiment a female catheter was used,  $\varnothing$ : 4.7mm (14Ch), length 18cm [Medicoplast International GmbH, Illingen, Germany].
- In the second experiment a Rusch Gold balloon catheter was used,  $\varnothing$ 5.3mm (16Ch), 5-15mL [Teleflex, Pennsylvania, USA]. The balloon was filled using a 10mL Luer tip (6%) emerald syringe [BD, New Jersey, USA].
- In the third experiment the same catheter as in experiment 1 was used, with a ultracover ultrasound probe cover (34 x 200 mm) [Ecolab, Minnesota, USA] wrapped around approximately the first 5 cm of the catheter. The probe cover was fixated using two rubber bands twisted around the cover and catheter tube.



(a) Filling of the phantom during the pilot of the experiment



(b) Leakage of the ultrasound gel as a result of overfilling of the phantom

Figure 6.1: Pilot experiment using the silicon rubber and PVA-hydrogel phantoms

## 6.2. Results

In Table 6.1 the results of the filling of the two phantoms with the different sets of instrumentation are shown. No results are shown for the experiment performed with the balloon catheter, since the test was deemed impractical. This will be further elaborated in the discussion in the next section.

The results show similar levels of filling, comparing the pilot test and the test with the catheter with the silicone phantom. The use of a catheter did already improve the amount of filling. A large increase in the filling percentage occurs for both phantoms when the concept using the probe cover is used. During the filling with the probe cover surrounding the catheter, the overfilling of the phantom could be easily seen from the outside of the phantom, as can be seen in Figure 6.2 and 6.3. And is most present in the figure of the silicone phantom.

Table 6.1: Results of phantom filling experiment

	Weight [g]	Volume [mL]	Estimated Volume [cm <sup>3</sup> ]	Filling percentage [%]
Pilot, silicone	22.13	21.70	24.0	90.4%
Pilot, PVA	27.64	27.10	28.1	96.4%
<b>1st experiment</b>				
Catheter, silicone	21.13	20.92	24.0	87.2%
Catheter, PVA	38.41	38.03	28.1	135.3%
<b>2nd experiment</b>				
Catheter with balloon, silicone	-	-	-	-
Catheter with balloon, PVA	-	-	-	-
<b>3rd experiment</b>				
Probe cover, silicone	34.31	33.97	24.0	141.5%
Probe cover, PVA	72.44	71.72	28.1	255.2%



Figure 6.2: Overfilling of the silicone phantom, during the experiment using the probe cover.



Figure 6.3: Overfilling of the PVA-phantom, during the experiment using the probe cover.

### 6.3. Discussion

Using the concept involving the use of a probe cover, increased the filling percentages of the silicone and PVA-hydrogel phantom by 54.3% and 119.9%, respectively. This clearly shows the potential of this concept, to be used as a method of sealing the vaginal cavity in real patients. An important factor for this experiment was only using materials and equipment used in the Erasmus Medical centre. This would ensure that concepts tested during this test could also be performed at the Erasmus MC, without the need for additional purchases. Another advantage would be that the staff is already familiar with the equipment used.

The experiment with the catheter with a balloon was aborted, as it was deemed impractical. The syringe with ultrasound gel was only friction-locked inside the catheter, applying the amount of pressure required to force the ultrasound gel to pass through the catheter, resulted in the syringe and catheter detaching. This resulted in a large spillage of the ultrasound gel, with some of the gel spilling outside the container positioned on the scale, which meant the amount of inserted ultrasound gel could not be monitored and verified anymore. After multiple unsuccessfully tries to avoid this uncontrolled spillage, the test was skipped due to being quite impractical. The experiment was performed under laboratory conditions without any time-pressure, or a patient which can block easy access and experiences discomfort. The procedure would probably turn out even more impractical with actual patients involved.

The experiment has proven that overfilling of the vaginal cavity inside both phantoms is possible. The ability of the probe cover to follow the shape of the anatomy, has not yet been tested. By performing this experiment again, and placing the filled phantoms inside a MR-scanner. The ability of the probe cover to follow the shape of the anatomy could be tested.

### 6.4. Conclusion

An experiment was performed to test methods for sealing the vaginal cavity, so that ultrasound gel can be used to fill the vaginal cavity improve the visibility of the vaginal cavity in MR-images. Two concept were tested against the first experiment to quantify the improvements. The concept using a female catheter with a balloon, was discarded due to being too impractical. The concept using a catheter surrounded by a probe cover showed great improvement in the filling percentage of both phantoms. This concept also allowed for overfilling of both phantoms. Additional testing, in which phantoms would be placed inside a MR-scanner, would provide data on the ability of the probe cover to follow the shape of the anatomy of the patient.

# 7

## Discussion

This chapter will provide a summary of the results presented in the previous chapters. Additionally, discussion on topics with an influence on multiple topics are presented.

### 7.1. Materials and testing

Both PVA-hydrogel and silicone rubber have been tested during this study to compare the mechanical properties against those of HAVW tissue. Silicone rubber was the closest match with the HAVW tissue. The range for the Young's modulus of 6.7 - 14.4 MPa, resulting from literature, was not reached by the samples used in this study. Silicon proved a closer match to the vaginal wall, compared to PVA-hydrogel. Calculated Young's moduli for silicone rubber were between 1.4 - 4.2 MPa, with 0.04 - 0.16 MPa for PVA-hydrogel.

The Young's modulus represents only part of the mechanical behaviour of a material. Other studies which provided stress-strain curves were compared with the most stiff samples found during testing. According to the comparisons made between the study of Martins et al. [1] and Chantereau et al. [2], silicone samples of type 3 tested with set-up 3, had similar stress-strain curves for certain window of strain.

### 7.2. Indentation testing and sample preservation

Indentation testing was performed as an alternative for tensile testing, due to being non-destructive. Comparing the results for different compositions of PVA-hydrogel (indentation test 1, and tensile test 2) showed similar patterns in the data collected between the two tests. Therefore, it was concluded that indentation testing could be a viable alternative to tensile testing.

Indentation testing with PA-hydrogel samples submerged in water for preservation, showed an increase in recorded hardness over time. This result affects the shelf life on a produced phantom, since the mechanical changes over time will influence mechanical properties of the phantom.

### 7.3. Phantom production

The surrounding tissue part of the phantom has not been studied during development. The current shape of this region was chosen based on ease of manufacturing and making the phantom easy to handle during testing. In the current phantom the volume of the surrounding tissue compared to the vaginal wall is multiple times larger. The mechanical properties of the different layer of the phantom, for both phantoms (PVA-hydrogel and silicone rubber), were different. However, these differences were probably larger compared to the difference in mechanical properties of the vaginal wall and the surrounding tissue. Thus the surrounding tissue is expected to have had a larger impact on the mechanical behaviour of the phantoms during testing.

To produce the phantom of silicone rubber, the viscosity of the rubber had to be lowered. This was done by the adding of silicone thinner during the manufacturing process. From the data of the indentation tests, the mechanical properties of the silicone rubber did show change due to the use of silicone thinner. Tensile testing was not performed with samples produced with silicone thinner. Therefore, the mechanical properties of the current silicone rubber phantom are unknown, and require additional testing to get an estimate.

## 7.4. Phantom testing

Phantom testing has been performed to compare the different methods for sealing the vaginal cavity, to fill the cavity with ultrasound gel for improved contrast in MR-imaging resulting in improved delineation of the vaginal cavity. One of the methods, female catheter with a balloon, was discarded due to proving impractical during testing. The other solution (wrapping a ultrasound probe cover around the catheter without a balloon) was compared against the test with just the catheter without a balloon. The results of testing showed a large difference between the two tests. Much more overfilling of the cavity was possible with the use of the method using the catheter surrounded by the probe cover.

The samples closest to the range from literature (6.7 - 14.4 MPa) had were pre-conditioned prior to tensile testing. These samples had gone through at least one prior tensile test before. However, consistent and repeatable pre-conditioning of a complete phantom can not be achieved easily.

## 7.5. Future testing

Future testing during development of the customized applicators, would include needle puncture testing with interstitial needles to validate the personalized needle applicator, and ultimately to quantify the difference in dose distributions that can be obtained with conventional and personalized applicators.

During this study, multiple criteria influencing the mechanical properties of a material have been noticed. Some of which have already been studied during the study, such as a pre-conditioning of samples prior to tensile testing and the influence of previous testing on the mechanical behaviour of samples. However, this often consisted of a single test to confirm an influence of these criteria, and not fully testing the influence. The influence of storage of PVA-hydrogel samples, has been noticed during indentation testing, but has not been testing using tensile testing to quantify the changes over time.

## 7.6. Conclusion

In this study the production process of a thin-walled double-layered phantom of the vaginal cavity has been developed and tested. This phantom can be used to test concepts developed for sealing the vaginal cavity. This is necessary so that ultrasound gel can be used to fill the vaginal cavity improve the visibility of the vaginal cavity in MR-images. The phantom consists of layer mimicking the vaginal wall, and a layer functioning as the surrounding tissue. Since the vaginal wall was considered most important, the study focused on this layer.

PVA-hydrogel and silicone rubber were selected as materials to test their ability to mimic the mechanical behaviour of the vaginal wall. Due to the surface properties of PVA-hydrogel, a specialized set-up was developed and used to perform tensile testing. During tensile testing, Young's moduli where calculated at different amounts of strain. The range for the Young's modulus of 6.7 - 14.4 MPa, resulting from literature, was not matched by the samples used in this study. Silicon proved a closer match to the vaginal wall, compared to PVA-hydrogel. Calculated Young's moduli for silicone rubber were between 1.4 - 4.2 MPa, with 0.04 - 0.16 MPa for PVA-hydrogel. Comparing the stress-strain curves instead of the calculated Young's moduli, resulted for silicone rubber samples, in similar stress-strain curves for certain window of strain.

Indentation testing was performed as an alternative for tensile testing, due to being non-destructive. And was confirmed as a possible alternative to tensile testing for the verification of mechanical properties of a material. Storage by submersion of PVA-hydrogel samples was shown to influence the mechanical properties over time, which has consequences for the shelf life of a produced phantom.

Two phantoms have been developed, from PVA-hydrogel and silicone rubber. The shape of these phantoms was based on delineated MR-images used in the study of Laan et al. [15], which were converted into 3D-structures. The 3D-structures have been used in the development of moulds, in which the phantoms were manufactured. During production, silicone thinner was required to lower the viscosity of the silicone rubber, in order to create the desired thin-walled structure of the vaginal wall. The use of silicone thinner decreases the stiffness of the silicone, when used during manufacturing. This was tested using indentation testing. The shape of the surrounding tissue was chosen to make the phantom easy to handle during testing.

To verify the usability of the phantom, the phantom along with samples were placed inside a MR-scanner, to compare intensity differences between the different materials used during this study. The results of this experiment concluded proper differences between different materials could be seen by untrained person. Differences between different composition of a similar material (silicone rubber and PVA-hydrogel) could be distinguished.

During the final experiment, the phantoms were tested to compare the different methods of sealing of the vaginal cavity. One of the methods, female catheter with a balloon, was discarded due to proving impractical during testing. The other solution (wrapping a ultrasound probe cover around the catheter without a balloon) was compared against the test with just the catheter. The results of testing showed a large difference between the two tests, the amount of filling of the vaginal cavity was improved by, 54.3% and 119.9%, for silicone rubber and PVA-hydrogel phantom respectively.



# A

## Tensile testing

In this appendix additional data on the different tensile tests are presented. This includes the data from the pilot (tensile test 1), the pre-load and maximum load measured during each test, graphs showing the course of Young's modulus along increasing amounts of strain.

### A.1. Pre-load and maximum load data

In this section the data on pre- and maximum load are shown for each tensile test with PVA-hydrogel samples. Results for the silicone rubber samples is not presented, due to the results being limited by the maximum load of the stage instead of the samples.

Table A.1: Pre-Load and maximum load values for tensile test 1 and 2.

PVA [%]	Cycli [-]	PreLoad [N]	SD [-]	Fmax [N]	SD [-]
<b>Tensile test 1</b>					
10	2	0.95	0.13	6.64	0.42
10	3	1.59	0.15	8.43	2.78
12	2	1.81	0.12	11.79	3.23
12	3	2.82	0.12	18.54	2.21
12	4	3.08	0.59	19.71	3.91
<b>Tensile Test 2</b>					
12	2	2.30	0.07	15.48	3.58
12	3	3.25	0.08	17.26	3.23
14	2	2.54	0.12	11.39	2.17
14	3	3.51	0.12	20.00	3.91
16	2	3.12	0.12	19.63	5.04
16	3	4.35	0.19	21.34	2.93

Table A.2: Pre-Load and maximum load values for tensile test 3, 4, 5, 8.

Tensile test [-]	PreLoad [N]	SD [-]	Fmax [N]	SD [-]
<b>Tensile test 3</b>	0.09	0.06	4.29	0.78
<b>Tensile test 4</b>				
Sample 1	0.12	0.026	11.77	2.376
Sample 2	0.12	0.019	5.89	1.009
<b>Tensile test 5</b>				
<b>Tensile test 5</b>	0.22	0.02	4.79	1.23
<b>Tensile test 8</b>				
<b>Tensile test 8</b>	0.06	0.05	3.54	1.78

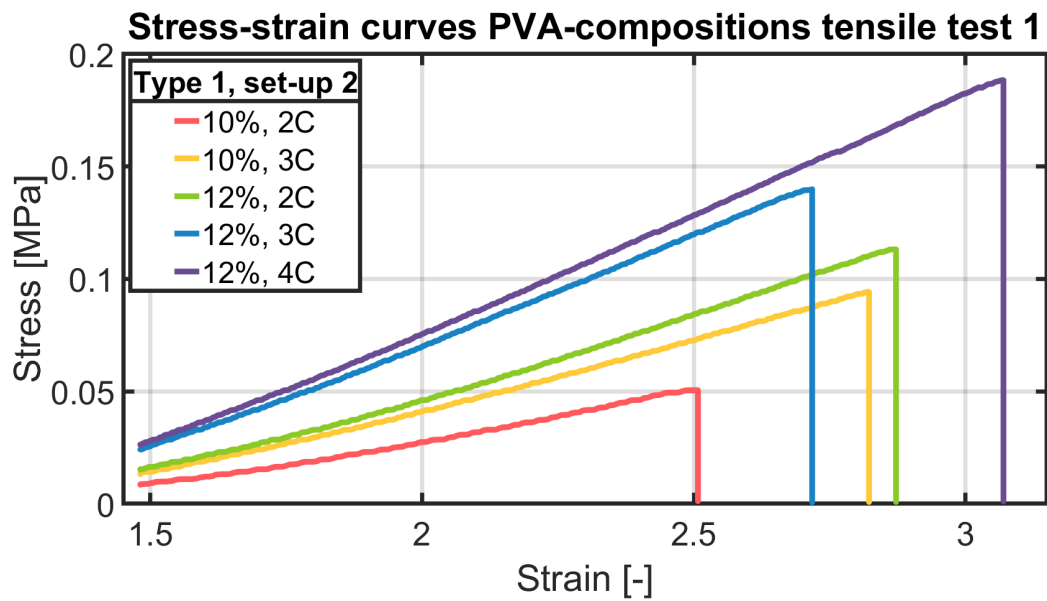
Tensile test 3, 4, 5, 8 were all based on 12% of PVA and 2 freeze-thaw cycles.

## A.2. Tensile test 1 (Pilot)

The results of the first tensile test, functioning as a pilot run, are presented below. This test was repeated in tensile test 2 with a larger range of PVA-compositions.

Table A.3: Results of tensile test 1.

PVA [%]	Cycli [-]	M1.5 [MPa]	SD [-]	M1.6 [MPa]	SD [-]	M1.7 [MPa]	SD [-]	M1.8 [MPa]	SD [-]	M1.9 [MPa]	SD [-]	M2.0 [MPa]	SD [-]
10	2	0.026	0.009	0.029	0.004	0.029	0.005	0.034	0.007	0.036	0.006	0.041	0.007
10	3	0.047	0.005	0.049	0.004	0.052	0.006	0.054	0.004	0.056	0.008	0.060	0.005
12	2	0.052	0.005	0.053	0.004	0.058	0.006	0.061	0.004	0.066	0.007	0.068	0.007
12	3	0.081	0.006	0.080	0.004	0.086	0.003	0.087	0.003	0.095	0.003	0.097	0.005
12	4	0.092	0.015	0.092	0.018	0.091	0.017	0.097	0.016	0.101	0.017	0.104	0.018



### A.3. Comparison PVA-samples

Figure A.2 show the results of tensile test 2. The development of the Young's modulus is shown as a function of the amount of strain of the sample. The dotted lines are not actually measured, and just a linear interpolation between the actual measured points indicated with the circles. The lines show clear differences between samples with the same % of PVA or same number of freeze-thaw cycles.

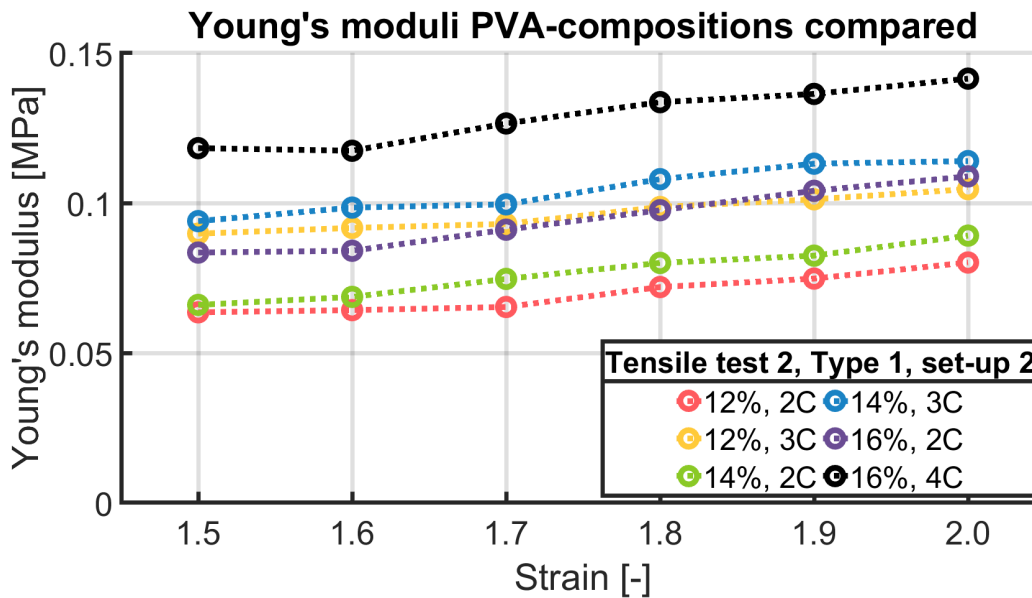


Figure A.2: Young's moduli comparison for tensile test 2.

### A.4. Tensile test 9

In Figure A.3 the stress-strain curves of all samples are shown. During this test the effects of plastic deformation of samples was tested. The curves show a behaviour similar to that of sample 3-5 from tensile test 7. Sample 1 and 2, which had been stretched multiple times, show no different behaviour compared to other samples.

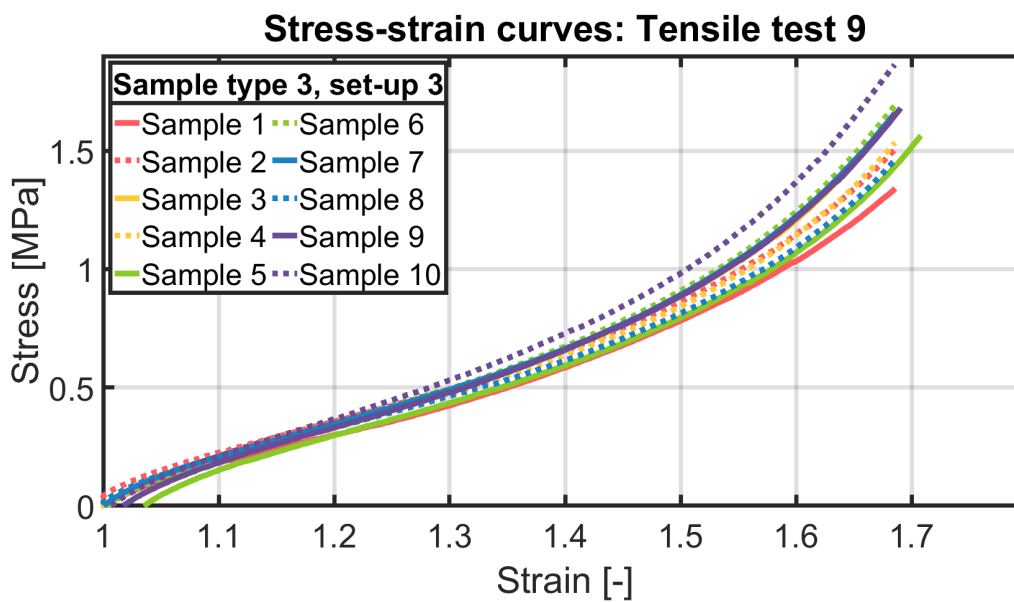


Figure A.3: Stress-strain curves: tensile test 9

### A.5. Tensile test 10

The graph below (Figure A.4) shows the data processing for a sample in tensile test 10 which is pre-strained three times. The data processing was adjusted to detect multiple starts and endings of the movement. The four starts detected in the image are indicated by the blue '+'-signs, the red signs indicate the detected endings of the movement of the stage.

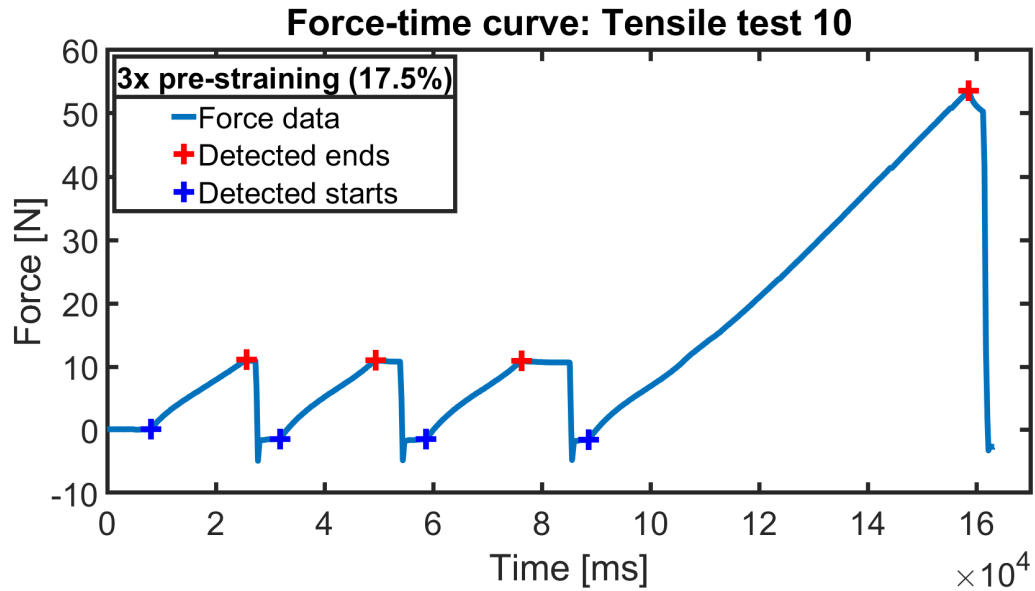


Figure A.4: Start and ending detection done by Matlab-code.

Tensile test 10 gave the opportunity to check the accuracy of the code/function which was used for the detection of the start and ending of the movement of the stage. During this test the stage made the same movement for the three pre-straining movements, the ends of these movements could be compared by zooming in on the plot and selecting the end points of each individual line. In Figure A.5 this is shown, comparing the two extremes (yellow and green line), results in a difference of 0.022mm which is considered accurate enough when measuring total movements of 35mm.

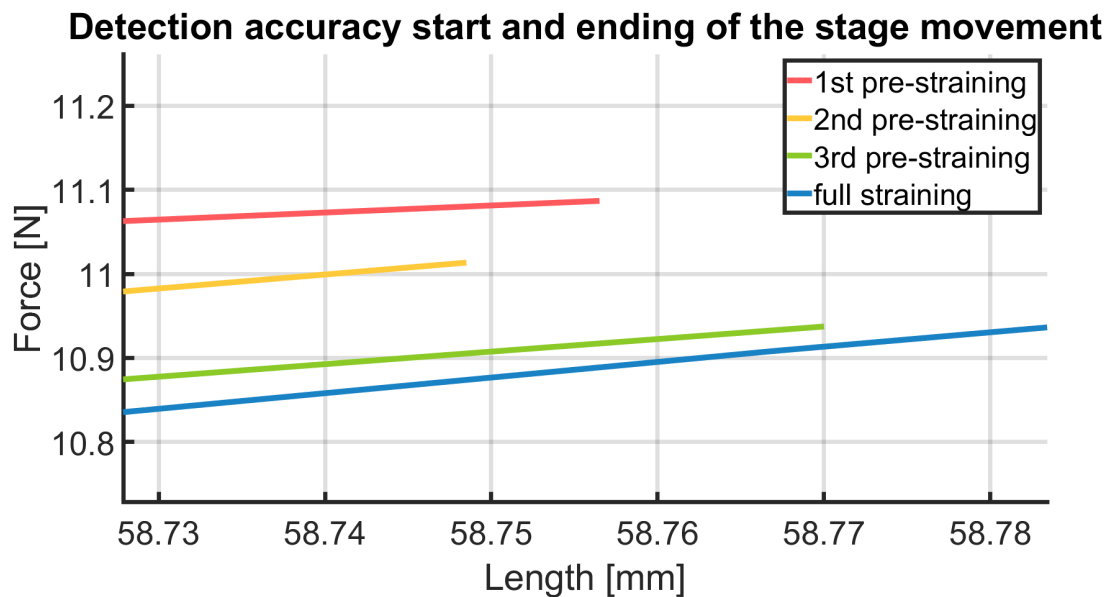


Figure A.5: Checking accuracy of the detection of the start and ending of the stage movement.

# B

## Indentation testing

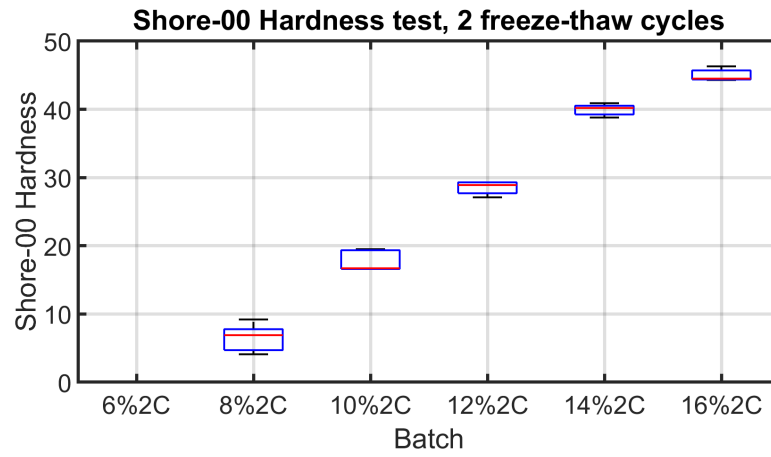
Additional data on the data collected during indentation testing is presented in this chapter. The data shown are the individual average measurements recorded during testing. Each data point in these tables represents nine separate measurements of which the measuring device calculated an average.

### B.1. Indentation test 1

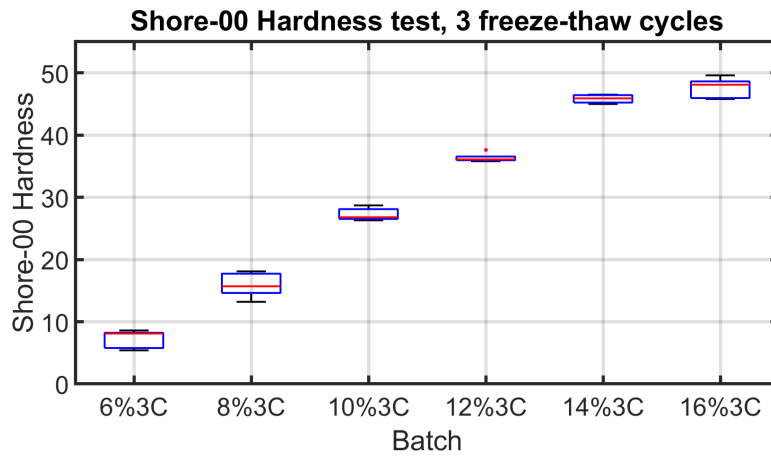
The measurements done during indentation test 1 are shown in Table B.1. This test was done to test whether the difference between compositions of PVA-hydrogel, tested in tensile test 2, could be detected as well with indentation testing. Similar to tensile test 2, the differences between samples with the same %-PVA or same number of freeze-thaw cycles can be clearly seen. In Figure B.1a, B.1b, B.1c, the hardness values for the samples with the same number of freeze-thaw cycles are compared.

Table B.1: Results of indentation test 1. Measurements (M1-M5) are average-value measurements consisting of 9 individual measurements each.

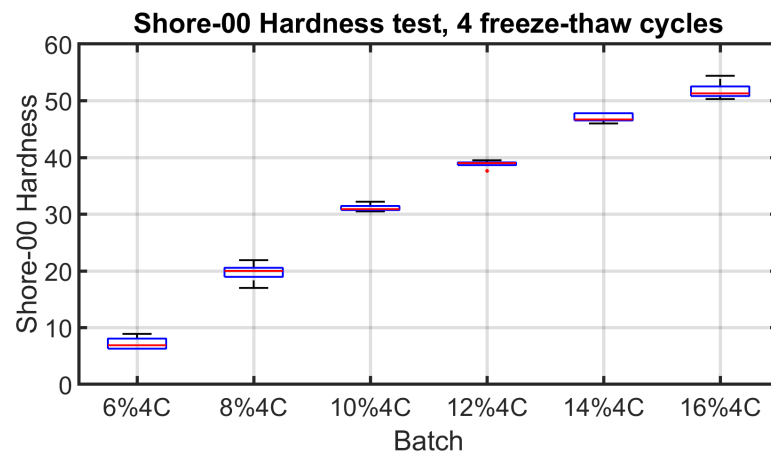
PVA [%]	Cycli [-]	Thickness [mm]	M1 [-]	M2 [-]	M3 [-]	M4 [-]	M5 [-]	Mean [-]	Average [-]	SD [-]
6	2	20.6	na	na	na	na	na	na	na	na
6	3	25.2	5.9	8.6	8.1	5.4	8.1	8.1	7.2	1.30
6	4	22.7	7.8	8.9	6.3	6.9	6.3	6.9	7.2	1.00
8	2	21.0	4.1	4.9	6.9	7.3	9.2	6.9	6.5	1.81
8	3	19.8	17.6	15.1	18.1	15.7	13.2	15.7	15.9	1.77
8	4	22.7	20.0	21.9	19.6	20.1	17.0	20.0	19.7	1.57
10	2	24.0	19.3	19.5	16.6	16.7	16.6	16.7	17.7	1.36
10	3	21.0	27.9	28.7	26.8	26.6	26.3	26.8	27.3	0.90
10	4	21.3	32.2	30.9	31.2	30.5	30.8	30.9	31.1	0.58
12	2	23.1	29.3	29.3	28.9	27.1	27.9	28.9	28.5	0.87
12	3	19.9	37.6	36.0	36.1	36.2	35.8	36.1	36.3	0.64
12	4	18.5	39.0	39.0	39.5	37.6	39.0	39.0	38.8	0.64
14	2	25.1	40.2	40.9	39.4	40.4	38.8	40.2	39.9	0.75
14	3	20.9	45.0	45.9	46.5	46.4	45.3	45.9	45.8	0.59
14	4	22.8	47.8	46.7	46.0	47.8	46.7	46.7	47.0	0.70
16	2	22.0	46.3	44.5	44.3	45.5	44.4	44.5	45.0	0.78
16	3	21.9	46.0	48.3	45.8	49.6	48.1	48.1	47.6	1.45
16	4	19.4	54.4	51.0	51.3	50.3	51.9	51.3	51.8	1.41



(a) Comparison for 2 freeze-thaw cycles.



(b) Comparison for 3 freeze-thaw cycles.



(c) Comparison for 4 freeze-thaw cycles.

Figure B.1: Comparison of the difference in hardness between samples with similar number of freeze-thaw cycles.

## B.2. Indentation test 2

Indentation test 2 monitored the progress of the hardness of two PVA-samples over time while being stored in water. The results of the test are presented in Table B.2.

Table B.2: Results of indentation test 2. Measurements are average-value measurements consisting of 9 individual measurements each.

Sample 1	06-11	07-11	08-11	09-11	13-11	20-11	27-11
M1	9.5	9.0	9.7	8.4	10.0	13.6	13.5
M2	9.0	8.3	9.6	8.1	10.1	10.0	13.4
M3	8.1	8.0	9.7	7.8	9.1	10.9	13.1
M4	6.8	7.5	8.8	8.7	7.3	10.5	12.9
M5	7.5	7.9	10.2	8.5	9.3	9.9	13.0
<b>Mean</b>	8.2	8.1	9.6	8.3	9.2	11.0	13.2
<b>St. dev.</b>	1.1	0.6	0.5	0.4	1.1	1.5	0.3

Sample 2	06-11	07-11	08-11	09-11	13-11	20-11	27-11
M1	30.1	29.6	29.4	28.1	28.9	31.3	31.6
M2	29.5	28.9	28.9	29.4	29.2	31.0	31.5
M3	29.2	29.6	30	28.6	29.0	30.2	32.0
M4	29.1	28.5	29.2	29.2	29.5	30.5	32.3
M5	29.3	28.7	28.9	29.1	29.4	30.1	31.0
<b>Mean</b>	29.4	29.1	29.3	28.9	29.2	30.6	31.7
<b>St. dev.</b>	0.4	0.5	0.5	0.5	0.3	0.5	0.5



# C

## PVA-hydrogel & silicone rubber production

In this appendix additional data is presented on the production of PVA-hydrogel and silicone rubber, including the production procedures. As well as measured compounds for each batch are presented.

### C.1. Standard procedure PVA-hydrogel production

Choices and variations in the production process of PVA-hydrogel greatly influences the mechanical properties of the PVA-hydrogel. Only two variations were introduced in the production, weight-percentage (w-%) PVA-powder and number of freeze-thaw cycles, while the rest of the production was kept as similar as possible for each batch of PVA-hydrogel. In order to achieve this, a standard procedure was used to produce the PVA-hydrogel, this procedure is adopted from the study of de Jong et al. [19].

#### C.1.1. Preparation PVA-hydrogel

First, the different ingredients are weighed, water, cooling liquid and PVA-powder. The % of PVA used determines the amount of water and cooling liquid required, these two are added in a ratio of 3:2. Secondly, these ingredients are mixed in a beaker, using a magnetic stirrer at a speed of 300 RPM (for % of PVA used < 12%) and 250 RPM (for % of PVA used  $\geq$ 12%). The mixture is heated to 93°C and kept at this temperature for 30 minutes, during this process the beaker is covered using a sheet of aluminium foil, this speeds up the heating and prevents the evaporation of the water. After the 30 minutes, the sheet of aluminium foil is removed and the mixture is left to cool for 20 minutes, cooling it to 50-65 °C (depended on batch and beaker size). During both heating and cooling the mixture is being stirred magnetically. After the cooling of the mixture, the mixture is poured into a mould, either directly from the beaker or with the use of a 20ml syringe. The mould closed by a cover and is placed in the freezer for 18 hours, after this period the mould is placed outside the freezer for 8 hours to thaw the sample back to room temperature. This last step is repeated according to the chosen amount of freeze-thaw cycles.



Figure C.1: Production of PVA-hydrogel, pink color is due to the used cooling liquid.

#### C.1.2. Preservation of samples

After the completion of at least one complete freeze-thaw cycle, the samples are removed from the mould. Remaining freeze-thaw cycle(s) are completed inside a plastic container. Periods in which the 24-hour cycle (freeze + thaw) was not possible due to lack of access to the facilities (e.g. weekends), the samples were kept inside a fridge before the remaining freeze-thaw cycles were completed. After the completion of all freeze-thaw cycles the samples are placed in plastic container filled with regular tap water for preservation of the samples. The plastic container is stored in a fridge, until the samples are needed for testing.

### C.1.3. Materials & equipment

The following materials and instruments were used in the production of the PVA-hydrogel:

- **Water**, regular tap water
- **Cooling liquid**, C&C automotive Type D/G12 [Jodima bvba, Kampenhout, Belgium]
- **PVA-powder**, Mw 89.000-98.000, 99+% hydrolyzed PVA [Sigma-Aldrich inc., St. Louis, Missouri, USA]
- **Beaker** Kimax Kimble No. 64000 [DWK Life Sciences GmbH, Mainz, Germany]
- **Weighing**, a Kern EMB 600-2 scale [Kern & Sohn GmbH, Balingen, Germany]
- **Mixing & heating**, a IKA C-MAG HS 7 control heat plate [IKA England Ltd., Oxford, United Kingdom]
- **Freezer** Liebherr GT 1432-20 [Liebherr GmbH, Bulle, Switzerland]

### C.2. Data PVA-hydrogel batches

In this section the data on the weighed compounds used for each batch of PVA-hydrogel are presented, along with the batch sizes and the weight before and after the preparation. Table C.1 shows each batch of PVA which was used for the production of tensile samples.

Table C.1: PVA-hydrogel batches tensile test 1-5, and 8

Batch	Water [g]	CL [g]	PVA [g]	Batch size [g]	$W_{start}$ [g]	$W_{end}$ [g]
<b>Tensile test 1</b>						
10%, 2&3C	81.00	54.01	15.02	150	274.04	265.49
12%, 2&3C	79.21	52.82	18.05	150	281.37	270.06
12%, 4C	79.22	52.79	18.02	150	281.29	267.82
<b>Tensile test 2</b>						
12%, 2&3C	105.59	70.40	23.99	200	331.42	307.56
14%, 2&3C	128.99	85.99	35.02	250	381.11	369.07
16%, 2&3C	125.99	84.06	39.99	250	381.16	368.53
Tensile test 3	79.22	52.81	18.01	150	281.56	268.34
Tensile test 4	105.61	70.39	24.02	200	331.30	318.32
Tensile test 5	105.61	70.40	23.99	200	330.93	320.90
Tensile test 8	105.60	70.40	24.01	200	331.73	317.71

Tensile test 3, 4, 5 and 8 were all based on 12% of PVA and 2 freeze-thaw cycles.

The data in Table C.2 shows all batch parameters for the samples used during indentation testing using PVA-hydrogel sample. The samples of indentation test 2 were part of larger batches used during tensile testing and the production of a MRI-sample.

Table C.2: PVA-hydrogel batches indentation test 1 and 2

Batch	Water [g]	CL [g]	PVA [g]	Batch size [g]	$W_{start}$ [g]	$W_{end}$ [g]
<b>Indentation test 1</b>						
6%	84.80	56.50	9.00	150	281.35	270.92
8%	82.76	55.23	12.01	150	281.24	268.39
10%	81.02	53.98	15.02	150	281.08	268.22
12%	79.23	52.81	18.03	150	281.29	271.88
14%	77.43	51.59	21.02	150	281.04	264.82
16%	75.60	50.40	23.99	150	281.28	268.34
<b>Indentation test 2</b>						
Sample 1: 12%, 2C	105.60	70.40	24.01	200	331.73	317.71
Sample 2: 14%, 3C	57.33	28.68	14.02	100	220.80	212.37

Sample 1 and 2 of indentation test 2 were part of the batches for tensile test 8 and 2-layer MRI core, respectively.

Table C.3 shows the batch parameters of the the produced phantom as well as the MRI-samples.

Table C.3: PVA-hydrogel batches MRI-samples and the phantom

Batch	Water [g]	CL [g]	PVA [g]	Batch size [g]	$W_{start}$ [g]	$W_{end}$ [g]
<b>MRI</b>						
14%, 3C	156.38	15.65	28.02	200	331.78	320.18
8%, 2C	83.64	8.35	8.00	100	220.75	212.00
<b>2-layer MRI</b>						
Core 14%, 3C	57.33	28.68	14.02	100	220.80	212.37
8%, 2C	122.68	61.32	16.02	200	331.52	320.25
<b>Phantom</b>						
VW 14%, 3C	57.35	28.64	13.99	100	231.21	213.43
ST 8%, 2C	245.32	122.68	32.00	400	687	647

### C.3. Silicone rubber production

Silicone rubber production is done according to the instructions provided by the manufacturer [24], [25]. The compounds (Part A, Part B, and thinner) are weighted using a scale with a precision of 0.01g. Part A of the silicone-compounds is weighed first, since this compound could not be dosed precisely because of the high viscosity of the material. Mixing is performed in a plastic container using a wooden stick to stir the compounds. During the production of the silicone rubber, latex-free gloves were worn, to prevent any contamination of the silicone rubber which could alter the curing process of the rubber.

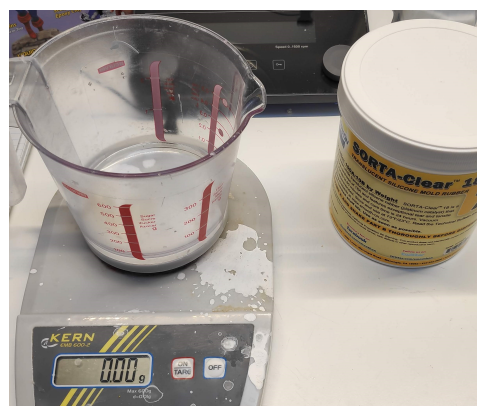


Figure C.2: Mixing container used for the production of silicone rubber.

#### C.3.1. Materials & equipment

The following materials and instruments were used in the production of silicone rubber:

- **Silicone rubber**, Smooth-Sil™940 and SORTA-Clear™18, [Smooth-on inc, Macungie, PA, USA]
- **Thinner**, Silicone Thinner™[Smooth-on inc, Macungie, PA, USA]
- **Mixing container**, plastic measuring beaker
- **Weighing**, a Kern EMB 600-2 scale [Kern & Sohn GmbH, Balingen, Germany]

### C.4. Data PVA-hydrogel batches

The weighted compounds used for the production of the silicone rubber samples used for tensile testing. Since the tensile tests were not destructive with silicone rubber samples due to the limitations of the stage used, samples could be reused between tests.

Table C.4: Silicone rubber tensile test 6,7,8 and 10

Batch	Brand	Part A [g]	Part B [g]	Thinner [g]	Batch size [g]
Tensile test 6, 7, 9	Smooth-Sil 940	160.91	16.10	-	177
Tensile test 10	Smooth-Sil 940	165.32	16.51	-	182

All batch parameters for the production of the silicone phantom and the MRI-samples.

Table C.5: Silicone rubber batches MRI-samples and the phantom

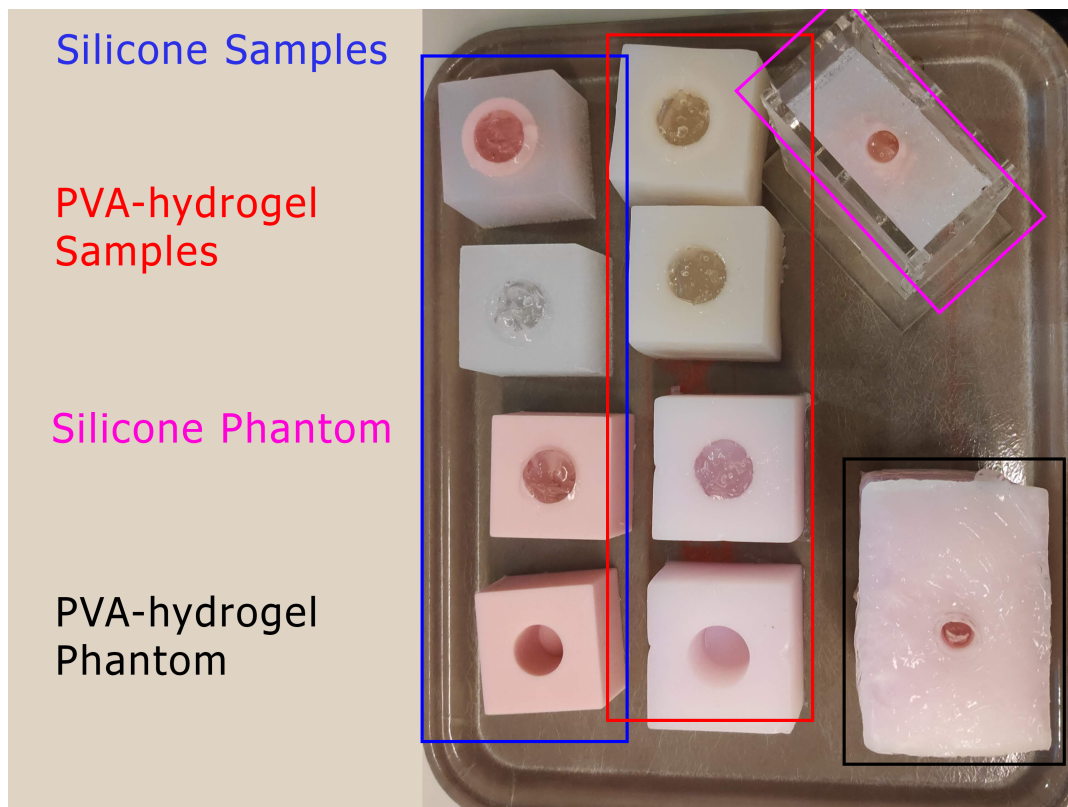
Batch	Brand	Part A [g]	Part B [g]	Thinner [g]	Batch size [g]
<b>MRI</b>					
Unclear samples	Smooth-Sil 940	163.22	16.35	-	180
Clear sample	Sorta-clear 18	156.99	15.65	-	173
<b>2-layer MRI</b>					
Core	Smooth-Sil 940	56.15	5.81	-	62
Surrounding	Sorta-clear 18	156.99	15.65	-	173
<b>Phantom</b>					
VW	Smooth-Sil 940	61.78	6.24	6.78	75
ST	Sorta-clear 18	147.67	14.96	16.27	179

VW: Vaginal wall, ST: Surrounding tissue

# D

## MRI-Experiment

In Table D.1 the individual measurements performed during the MRI-experiment are presented. Measurements were performed using the viewing software included with the made MR-images. Measurements were performed by placing circles in the MR-image, the software would subsequently perform the calculations automatically. Each calculation resulted in a maximum, average, and standard deviation value for the intensity of the pixels within the placed circle.



Positions of the groups of both materials are shown in the image. The individual samples of each material are, from top to bottom:  
Double layered sample, filled with ultrasound gel.  
8%, 2C for PVA, and Sorta Clear 18 for silicone rubber, filled with ultrasound gel.  
14%, 3C for PVA, and Smooth-sil 940 for silicone rubber, filled with ultrasound gel.  
14%, 3C for PVA, and Smooth-sil 940 for silicone rubber, empty.  
Both phantoms were filled with ultrasound gel.  
The positions of the samples matches those of Figure 4.2.

Figure D.1: Positioning of the sample used in the MR-scanner.

Table D.1: Results of the intensity measurements performed on the MR-images.

Silicon	Max	Av	SD	PVA-hydrogel	Max	Av	SD
Core 1 (Air)	327.0	267.7	18.1	Core 1 (Air)	346.0	270.2	26.7
	327.0	266.8	18.2		407.0	286.7	31.8
	314.0	265.2	15.5		344.0	279.7	24.8
Sample 1	456.0	411.8	20.7	Sample 1	2051.0	2005.0	31.7
	506.0	444.9	25.2		1867.0	1776.9	51.2
	523.0	476.5	23.2		1917.0	1811.7	55.3
Core 2 (UG) (air pocket present)	1205.0	867.7	277.0	Core 2 (UG)	1565.0	1283.6	116.7
	1273.0	899.4	264.8		1708.0	1316.0	113.2
	1387.0	921.8	279.6		1463.0	1311.5	72.5
Sample 2	555.0	497.7	24.7	Sample 2	2089.0	2012.0	32.8
	561.0	492.2	28.0		2086.0	1974.5	46.9
	595.0	480.2	35.8		1966.0	1925.9	22.0
Core 3 (UG) (air pocket present)	1273.0	1039.8	173.0	Core 3 (UG)	1393.0	1274.8	66.7
	1278.0	1016.3	227.8		1398.0	1278.6	57.3
	1273.0	1035.6	164.3		1425.0	1264.7	71.5
Sample 3	807.0	694.6	52.9	Sample 3	1646.0	1475.8	47.7
	749.0	672.0	32.9		1670.0	1564.3	39.8
	791.0	711.4	37.9		1708.0	1639.1	32.9
Core 4 (UG) (air pocket present)	1098.0	861.1	169.8	Core 4 (UG)	1349.0	1048.7	104.7
	1126.0	918.3	113.8		1548.0	1090.1	94.1
	1098.0	913.5	118.1		1364.0	1084.3	77.4
Sample 4	628.0	516.9	44.2	Sample 4	1568.0	1385.8	73.8
	754.0	660.5	41.0		1421.0	1334.5	36.9
	733.0	647.7	35.3		1407.0	1290.9	36.7
Extra layer 4	527.0	433.7	47.8	Extra layer 4	1709.0	1581.3	75.4
	735.0	491.3	93.2		1763.0	1611.5	158.5
	483.0	424.6	31.2		1775.0	1669.3	75.7
Phantom silicon	Max	Av	SD	Phantom PVA	Max	Av	SD
Core (UG)	1115.0	911.2	130.6	Core (UG)	1343.0	1167.9	76.3
	1184.0	873.9	233.1		1290.0	1130.8	74.2
	1115.0	920.6	128.6		1212.0	1087.4	71.1
VW	981.0	601.2	204.6	VW	2022.0	1694.2	311.7
	908.0	635.4	118.3		1845.0	1610.9	277.2
	934.0	615.4	186.5		1977.0	1733.0	244.0
Sample	874.0	781.4	47.6	Sample	1634.0	1564.5	34.3
	814.0	715.6	44.6		1805.0	1756.4	23.4
	997.0	821.5	56.5		1659.0	1554.9	51.4

# E

## Mould design

In this appendix additional information on the moulds produced and used during this study is presented. Beginning with the mould developed for the manufacturing of the tensile samples. The samples including their dimensions are shown in Figure E.1.

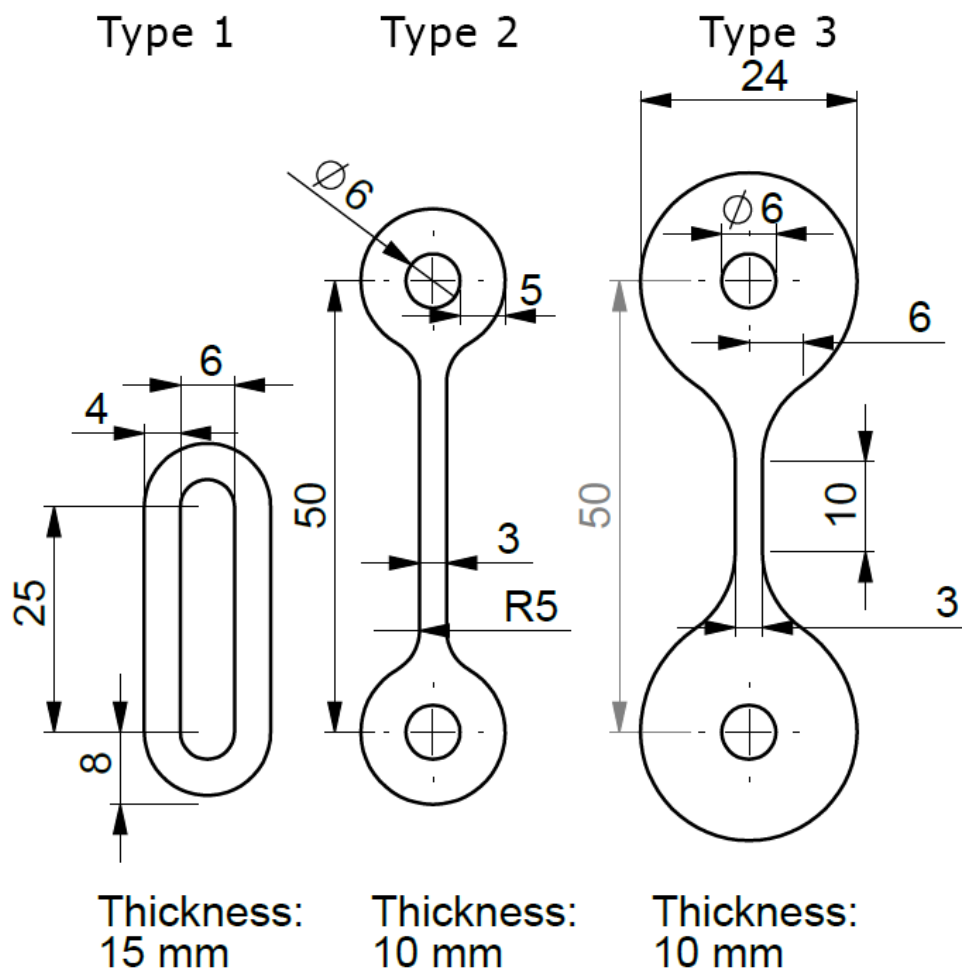


Figure E.1: Dimensions of the different sample types

## E.1. Mould tensile testing

For the tensile testing, samples were required to have a consistent shape which suitable for testing. Due to the low stiffness and slippery surface properties of PVA-hydrogel, samples can not be manufactured using subtractive manufacturing, and additive manufacturing is required. Since the PVA-hydrogel is in a liquid state before the freeze-thaw process is started, pouring the PVA-hydrogel in a mould to create the desired shape is the most optimal method of sample production. Manufacturing of the samples were made using 3D-printed moulds, which were designed and converted into STL-files using Solidworks 2019 [Dassault Systèmes, Vélizy-Villacoublay, France]. The STL-files were converted into G-code by Cura 4.7 [Ultimaker, Geldermalsen, the Netherlands], and printed using a Ultimaker 3 [Ultimaker, Geldermalsen, the Netherlands]. The double layered top cover was cut from 4mm sheets of acrylic, cutting was performed by a Lion 30W laser cutter [Lion Laser Systems BV, Breda, the Netherlands]. All moulds were designed to consist of different modular parts, this made upgrading the mould, swapping sub-parts, and the removal of the samples from the mould easier. Instead of directly removing the samples from the mould, the inner parts (creating the holes within each sample) were removed first, reducing the change of rupturing a sample during the removal from the mould. Each mould was designed to produce ten sample simultaneously.



Figure E.2: Air defects influencing the shape of tensile sample of type 1.

### E.1.1. Mould type 1

The mould for type 1 samples was developed prior to the development of the other moulds. The design underwent multiple iterations to optimize the samples produced by the mould. The mould consisted of a bottom part, forming the outer shape of each sample, the inner shape was formed by insertable middle parts which were held in place using 2 pin hole connections. First batches were produced without a top cover in place during the filling of the mould, however this was changed due to sample shrinkage and to reduce surface defects, as can be seen in Figure E.2. A new top cover was developed with another set of pin hole connections on top of the bottom part of the mould and on top of each middle part formed the fixation of the mould. To further fixate the top cover and reduce the amount of leakage between different layers tape was used. Additionally two holes were added above each part of the mould, which would produce a single sample, to allow for the filling of the mould and the escaping of air during the filling of the mould. The mould was fully assembled and fixated before the PVA-hydrogel was inserted into holes in the top cover, overfilling was performed to reduce the amount of surface defects due to trapped air. Figure E.3 shows the mould type 1 fully assembled, before the additional fixation with tape.

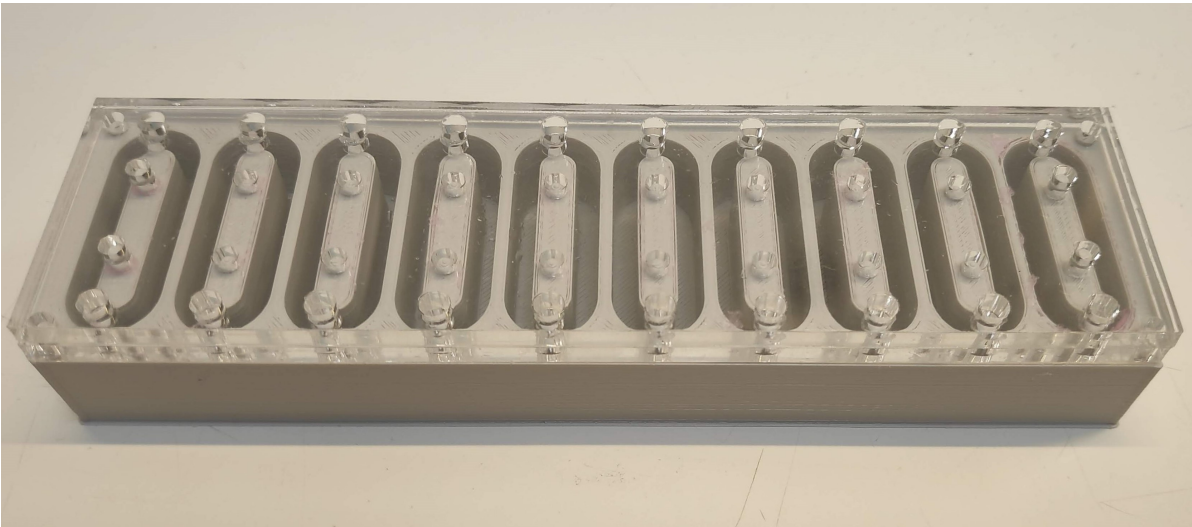


Figure E.3: Mould for the manufacturing of samples of type 1.

### E.1.2. Mould type 2 and 3

The main differences between these moulds and the mould for type 1 samples are:

- The depth of bottom part of the mould is reduced from 15mm to 10mm.
- Instead of a single inserted middle part, now two parts are used, due to the shape of the sample no longer having a open connection between the fixation points.
- The cavities are not placed in a single line, but in a zig-zag pattern to reduce overall size of the mould.

Figure E.4 shows the mould type 2, filled with a batch of samples. The samples are all connected through a thin film, this film was trimmed as much as possible prior to tensile testing.



Figure E.4: Mould for the manufacturing of samples of type 2.

Figure E.5 shows the mould type 3 with some of the samples already removed from the mould.

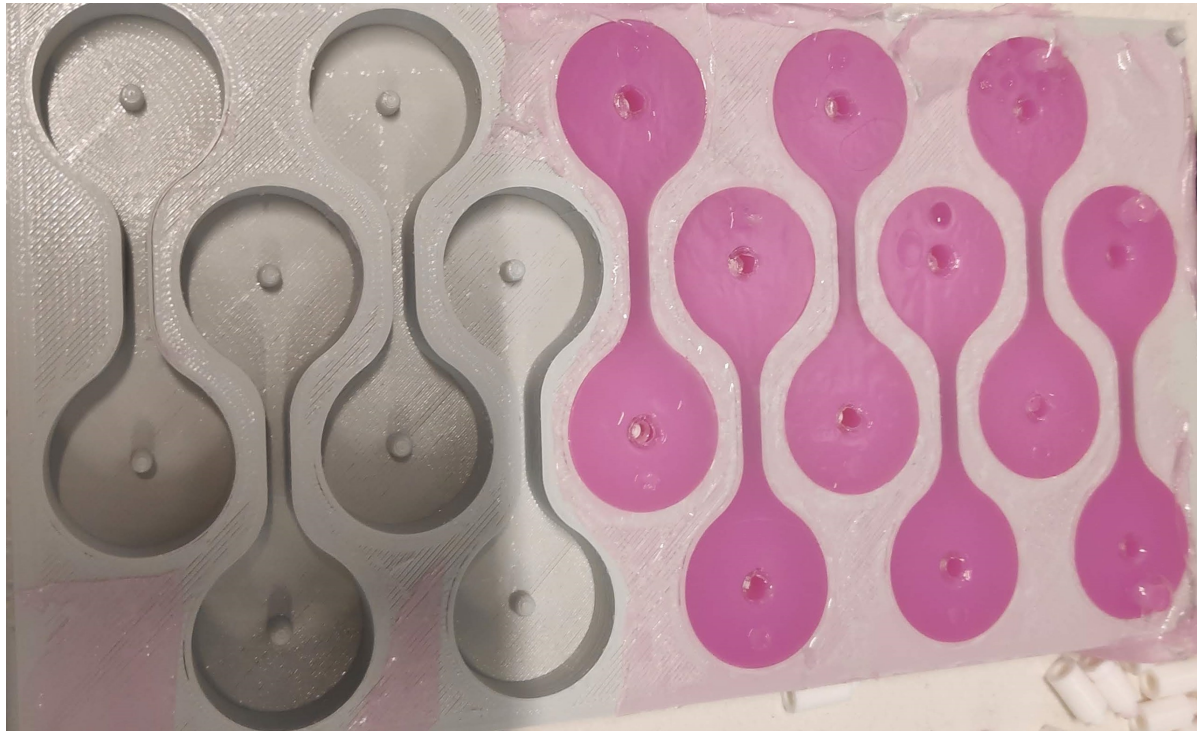


Figure E.5: Mould for the manufacturing of samples of type 3.

## E.2. Phantom mould

To produce a phantom, two moulds are required, the first is used for the manufacturing of the layer mimicking the vaginal wall, the second layer mimics the surrounding tissue. The mould for the manufacturing of the vaginal wall has had multiple design iterations before its final design. Initially, the mould was designed to consist of only two halves instead of four parts, however this made the fitting and positioning of the water-soluble insert rather difficult. With a new mould consisting of four parts, the insert used formfitting to remain in place, however due to the tolerances required for 3D-printing this did not result in a tight fit.

Further iterations introduced bolts which could be used for the fixation and positioning of the insert inside the mould, and the introduction of filling channels in the top part of the mould. These channels were added to create a wider path for the silicone to fill the mould, due to the high viscosity filling the mould at the top was not possible with silicone rubber. However, these channels did not solve the issue of filling the mould with silicon. To fully resolve the issues related to the viscosity of the silicone rubber, both a thinner was added to the silicone rubber and the number of filling channels was increased to four with the beginning of each channel a small basin which could be filled which would feed a continuous supply of silicone rubber into the mould. These four basins can be seen filled in Figure 5.4. Air could escape during the filling process through the space between the mould and the insert at the top of the mould.

# F

## Clinical background

### F.1. Stages of cervical cancer

The progression of the disease is measured in both cancer spread and tumor growth and divided into stages, the FIGO stages. The scale is developed by the Fédération Internationale de Gynécologie et d'Obstétrique (International Federation of Gynaecology and Obstetrics). The main difference between the different stages is the size of the tumor and whether or not the tumor has spread to (certain) organs. A complete table with descriptions of every (sub)stage can be seen in the table below.

Table F1: The FIGO stages of the progression of cervical cancer [3]

Stage	Description
I	Spread from the cervix lining into the deeper tissue but is still just found in the uterus. No spread to other parts of the body.
IA	The cancer is diagnosed only by viewing cervical tissue or cells under a microscope. Imaging tests or evaluation of tissue samples can also be used to determine tumor size.
IA2	There is a cancerous area 3 mm to less than 5 mm in depth.
IB	In this stage, the tumor is larger but only confined to the cervix. No distant spread.
IB1	The tumor 5 mm or more in depth and less than 2 centimeters (cm) wide.
IB2	The tumor is 2 cm or more in depth and less than 4 cm wide.
IB3	The tumor is 4 cm or more in width.
II	The cancer has spread beyond the uterus to nearby areas, such as the vagina or tissue near the cervix, but it is still inside the pelvic area. No spread to other parts of the body.
IIA	The tumor is limited to the upper 2/3 of the vagina. No spread to the parametrial area.
IIA1	The tumor is less than 4 cm wide.
IIA2	The tumor is 4 cm or more in width.
IIB	The tumor has spread to the parametrial area. The tumor does not reach the pelvic wall.
III	The tumor involves the lower 1/3 of the vagina, and/or spread to the pelvic wall, and/or swelling of the kidney and/or involves regional lymph nodes. No distant spread.
IIIA	The tumor involves the lower third of the vagina, but no grown into the pelvic wall.
IIB	The tumor has grown into the pelvic wall and/or affects a kidney.
IIIC	The tumor involves regional lymph nodes. Detection possible by imaging tests or pathology.
IIIC1	The cancer has spread to lymph nodes in the pelvis.
IIIC2	The cancer has spread to para-aortic lymph nodes. These lymph nodes are found in the abdomen near the base of the spine and near the aorta, a major artery runs from the heart to the abdomen.
IVA	The cancer has spread to the bladder or rectum, no spread to other parts of the body.
IVB	The cancer has spread to other parts of the body.



# G

## Phantom testing

In Table G.1, G.2, G.3, G.4, G.5, and G.6, the measurements performed during each experiment are shown. The first result in each table indicated as 'difference', was used as the result of the test. The other results indicated with 'difference' in each table, were used to verify the measurements. The difference between the two values is due to overfilling of the phantom (residue weight) or the used equipment.

Table G.1: Weight measurements phantom filling experiment with the silicon phantom and the pilot set-up.

Instrument	Weighing moment	Weight [g]
Phantom	Before experiment	133.05
	After experiment	155.18
	<b>Difference</b>	22.13
Syringe	Before experiment	75.39
	After experiment	47.64
	<b>Difference</b>	27.75
Scale	Before experiment	133
	After experiment	160
	Residue weight	6

Table G.2: Weight measurements phantom filling experiment using the PVA-hydrogel phantom and the pilot set-up.

Instrument	Weighing moment	Weight [g]
Phantom	Before experiment	306.72
	After experiment	334.36
	<b>Difference</b>	27.64
Syringe	Before experiment	77.84
	After experiment	37.28
	<b>Difference</b>	40.56
Scale	Before experiment	307
	After experiment	347
	Residue weight	13

Table G.3: Weight measurements phantom filling experiment with the silicon phantom and the catheter without balloon set-up.

Catheter without balloon, silicon		
Instrument	Weighing moment	Weight [g]
Phantom	Before experiment	134.73
	After experiment	155.86
	<b>Difference</b>	21.13
Syringe	Before experiment	77.68
	After experiment	36.09
	<b>Difference</b>	41.59
Scale	Before experiment	135
	After experiment	176
	Residue weight	18
Catheter	Before experiment	3.71
	After experiment	6.43
	<b>Difference</b>	2.72

Table G.5: Weight measurements phantom filling experiment with the silicon phantom and the condom set-up.

Catheter with condom, silicon		
Instrument	Weighing moment	Weight [g]
Syringe	Before experiment	92.85
	After experiment	58.11
	<b>Difference</b>	34.74
Catheter	Before experiment	5.93
	After experiment	40.24
	<b>Difference</b>	34.31
Phantom	Before experiment	134.40
	After experiment	188.47
	<b>Difference</b>	54.07
Scale	Before experiment	134
	After experiment	175
	Residue weight	0
Clamp	-	13.57

Table G.4: Weight measurements phantom filling experiment with the PVA-hydrogel phantom and the catheter without balloon set-up.

Catheter without balloon, PVA		
Instrument	Weighing moment	Weight [g]
Phantom	Before experiment	313.60
	After experiment	352.01
	<b>Difference</b>	38.41
Syringe	Before experiment	91.89
	After experiment	42.02
	<b>Difference</b>	49.87
Scale	Before experiment	314
	After experiment	364
	Residue weight	10
Catheter	Before experiment	3.69
	After experiment	6.02
	<b>Difference</b>	2.33

Table G.6: Weight measurements phantom filling experiment with the PVA-hydrogel phantom and the condom set-up.

Catheter with condom, PVA		
Instrument	Weighing moment	Weight [g]
Syringe	Before experiment	149.97
	After experiment	73.04
	<b>Difference</b>	76.93
Catheter	Before experiment	5.94
	After experiment	78.38
	<b>Difference</b>	72.44
Phantom	Before experiment	321.25
	After experiment	412.33
	<b>Difference</b>	91.08
Scale	Before experiment	321
	After experiment	416
	Residue weight	4
Clamp	-	13.60

# Bibliography

- [1] P. Martins, A. Lopes Silva-Filho, A. M. Rodrigues Maciel Da Fonseca, A. Santos, L. Santos, T. Mascarenhas, R. M. Natal Jorge, and A. J. Ferreira, “Biomechanical properties of vaginal tissue in women with pelvic organ prolapse,” *Gynecologic and Obstetric Investigation*, vol. 75, pp. 85–92, feb 2013.
- [2] P. Chantereau, M. Brieu, M. Kammal, J. Farthmann, B. Gabriel, and M. Cosson, “Mechanical properties of pelvic soft tissue of young women and impact of aging,” *International Urogynecology Journal*, vol. 25, pp. 1547–1553, oct 2014.
- [3] “Cervical Cancer: Stages | Oncology, American Society of Clinical.” <https://www.cancer.net/cancer-types/cervical-cancer/stages>. Accessed on: 2020-11-25.
- [4] World Health Organization, “Incidence, mortality and prevalence numbers for all types of cancer worldwide.” <http://gco.iarc.fr/today>, 2018. Accessed on: 2020-11-10.
- [5] R. Pötter, K. Tanderup, C. Kirisits, A. de Leeuw, K. Kirchheiner, R. Nout, L. T. Tan, C. Haie-Meder, U. Mahantshetty, B. Segedin, *et al.*, “The embrace ii study: The outcome and prospect of two decades of evolution within the gec-estro gyn working group and the embrace studies,” *Clinical and translational radiation oncology*, vol. 9, pp. 48–60, 2018.
- [6] “Estimated age-standardized incidence and mortality rates (World) in 2018, worldwide, both sexes, all ages | World Health Organization.” <http://gco.iarc.fr/today/online-analysis-multi-bars?v=2018>. Accessed on 2020-11-11.
- [7] A. Baah-Dwomoh, J. McGuire, T. Tan, and R. De Vita, “Mechanical Properties of Female Reproductive Organs and Supporting Connective Tissues: A Review of the Current State of Knowledge,” nov 2016.
- [8] R. Eberhart, C.-J. Chuong, and P. Zimmern, “Exploring biomechanical methods to study the human vaginal wall,” *Neurourology and Urodynamics*, vol. 36, pp. 499–506, feb 2017.
- [9] A. M. Ruiz-Zapata, A. J. Feola, J. Heesackers, P. de Graaf, M. Blaganje, and K. D. Sievert, “Biomechanical Properties of the Pelvic Floor and its Relation to Pelvic Floor Disorders[Figure presented],” apr 2018.
- [10] J. T. Goh, “Biomechanical properties of prolapsed vaginal tissue in pre- and postmenopausal women,” *International Urogynecology Journal*, vol. 13, no. 2, pp. 76–79, 2002.
- [11] L. Lei, Y. Song, and R. Q. Chen, “Biomechanical properties of prolapsed vaginal tissue in pre- and postmenopausal women,” *International Urogynecology Journal*, vol. 18, no. 6, pp. 603–607, 2007.
- [12] P. E. Zimmern, R. C. Eberhart, and A. Bhatt, “Methodology for biomechanical testing of fresh anterior wall vaginal samples from postmenopausal women undergoing cystocele repair,” *Neurourology and Urodynamics*, vol. 28, pp. 325–329, apr 2009.
- [13] S. O. Lopez, R. C. Eberhart, P. E. Zimmern, and C. J. Chuong, “Influence of body mass index on the biomechanical properties of the human prolapsed anterior vaginal wall,” *International Urogynecology Journal and Pelvic Floor Dysfunction*, vol. 26, pp. 519–525, apr 2015.
- [14] M. Ahearne, Y. Yang, and K.-K. Liu, *Mechanical Characterisation of Hydrogels for Tissue Engineering Applications*, vol. 4. 2008.
- [15] R. C. Laan, R. A. Nout, J. Dankelman, and N. J. van de Berg, “MRI-driven design of customised 3D printed gynaecological brachytherapy applicators with curved needle channels,” *3D Printing in Medicine*, vol. 5, p. 8, dec 2019.
- [16] R. C. Bump, A. Mattiasson, K. Bo, L. P. Brubaker, J. O. DeLancey, P. Klarskov, B. L. Shull, and A. R. Smith, “The standardization of terminology of female pelvic organ prolapse and pelvic floor dysfunction,” *American Journal of Obstetrics and Gynecology*, vol. 175, pp. 10–17, jul 1996.

- [17] G. Paradossi, F. Cavalieri, E. Chiessi, C. Spagnoli, and M. K. Cowman, "Poly(vinyl alcohol) as versatile bio-material for potential biomedical applications," in *Journal of Materials Science: Materials in Medicine*, vol. 14, pp. 687–691, aug 2003.
- [18] S. Jiang, S. Liu, and W. Feng, "PVA hydrogel properties for biomedical application," *Journal of the Mechanical Behavior of Biomedical Materials*, vol. 4, pp. 1228–1233, oct 2011.
- [19] T. L. de Jong, L. H. Pluymen, D. J. van Gerwen, G. J. Kleinrensink, J. Dankelman, and J. J. van den Dobbelsteen, "PVA matches human liver in needle-tissue interaction," *Journal of the Mechanical Behavior of Biomedical Materials*, vol. 69, pp. 223–228, may 2017.
- [20] K. Nattagh, T. Siau, J. Pouliot, I. C. Hsu, and J. A. Cunha, "A training phantom for ultrasound-guided needle insertion and suturing," *Brachytherapy*, vol. 13, pp. 413–419, jul 2014.
- [21] C. W. Swanick, K. O. Castle, L. A. Rechner, G. M. Rauch, A. Jhingran, P. J. Eifel, and A. H. Klopp, "Optimizing packing contrast for MRI-based intracavitary brachytherapy planning for cervical cancer," *Brachytherapy*, vol. 14, pp. 385–389, may 2015.
- [22] "Aquasonic ultrasound gel | Laboratories, Parker." <https://bio-medical.com/media/support/aquasonic-clear-technical-datasheet.pdf>. Accessed on: 2020-12-03.
- [23] "Supragel | Medical Products, LCH." <https://www.girodmedical.co.uk/contact-gel-ecg-supragel-lch.html>. Accessed on: 2020-12-30.
- [24] "SORTA-Clear™ 18 Product Information | Smooth-On, Inc." <https://www.smooth-on.com/products/sorta-clear-18/>. Accessed on: 2021-01-04.
- [25] "Smooth-Sil™ 940 Product Information | Smooth-On, Inc." <https://www.smooth-on.com/products/smooth-sil-940/>. Accessed on: 2021-01-04.